BCSD Downscaled Transient Climate Projections for Eight Select GCMs over British Columbia, Canada

—

Hydrologic Modelling Project

Final Report (Part I)

1 April 2011

Arelia T. Werner

University of Victoria

(BLANK)

Citation

About PCIC

Disclaimer

(BLANK)

Acknowledgements

(BLANK)

Preface

The Pacific Climate Impacts Consortium (PCIC) has completed a *Hydrologic Modelling* project with the aim of quantifying the hydrologic impacts of projected climate change in select British Columbia watersheds. The main objective of the Hydrologic Modelling project is to provide future projections of the impacts of climate change on monthly and annual streamflow in three BC watersheds for the 2050s: the Peace, Campbell and Columbia, with particular emphasis on sites corresponding to BC Hydro power generation assets. The Hydrologic Modelling Project utilized an ensemble of climate projections derived from several global climate models (GCMs) forced with three emissions scenarios, statistically downscaled to high spatial and temporal resolution, to force a hydrologic model. The output of this model was subsequently used to assess and analyze the projected hydrologic response to climate change.

Due to the scope of work required for this project, reporting is accomplished using two complementary, but independent, reports. The current report describes the methods used to derive the ensemble of statistically downscaled climate projections. It describes the GCM selection and statistical downscaling methodology in detail, discusses the validation of the statistical downscaling results, and presents general results of projected climate changes in British Columbia based on the derived projections. Although these climate projections were originally developed with the intent to generate hydrologic projections, we feel that these results are applicable to a broad range of impact studies and provide a valid understanding of the general consequences of projected climate change within British Columbia. Therefore, this report is also intended to make our results accessible to the wider scientific and operational audience. A companion report (Schnorbus et al. 2011)[1] provides a thorough summary of the results of the hydrologic modelling, specifically for the three study areas, and focusing mainly on the methods employed and results obtained from the hydrologic modelling exercise itself.

Analysis using updated data and peer-reviewed methodology has formed the basis of this work. Whenever possible, our intention was also to extend and improve upon existing results. Specifically, we have taken the opportunity to update the climate change projections originally presented by PCIC in the *Climate Overview 2007* report (Rodenhuis et al. 2009). Consequently, much of the discussion in the current document is structured for direct comparison to the Climate Overview 2007 report, adopting the same regional delineation for summarizing results. Improvements include selecting GCMs based on their performance globally and regionally, bias-correction of the GCM output, and statistical downscaling of the resultant projections to high spatial resolution (1/16° or ~ 6km). The result is a suite of high-resolution projections of daily minimum temperature, maximum temperature and precipitation from an ensemble of 23 climate projections encompassing a spatial domain that includes all of British Columbia, plus a small portion of the United States. A detailed description and inventory of forcing data is provided as an appendix to the companion report of Schnorbus et al. (2011).

The Hydrologic Modelling project is part of a larger *Hydrologic Impacts* research program that has been underway at PCIC to address the consequences of climate change on water resources in British Columbia (Rodenhuis et al. 2007)[2]. The research plan is composed of four distinct projects: *Climate Overview*, *Hydrologic Modelling* (the subject of the current report), *Regional Climate Modelling Diagnostics*, and *Synthesis*. The objectives of the Climate Overview are to identify the scope and intensity of the threat of potential impacts to water resources by climate variability and change in British Columbia (Rodenhuis et

---

[1] Schnorbus, M.A., K.E. Bennett, A.T. Werner and A.J. Berland, 2011: *Hydrologic Impacts of Climate Change in the Peace, Campbell and Columbia Watersheds, British Columbia, Canada*. Pacific Climate Impacts Consortium, University of Victoria, Victoria, BC, 157 pp.

[2] Rodenhuis, D., A.T. Werner, K.E. Bennett, and T.Q. Murdock, 2007: *Research Plan for Hydrologic Impacts*. Pacific Climate Impacts Consortium, University of Victoria, Victoria, BC, 34 pp.

al. 2009)[3]. The objective of the Regional Climate Modelling Diagnostics project is to validate the water balance of the Canadian Regional Climate Model (CRCM) in select BC watersheds, and to use the CRCM to simulate future climate and hydrologic conditions as a parallel effort to the Hydrologic Modelling project (Rodenhuis et al. 2011)[4]. Lastly, the purpose of the Synthesis project (Shrestha et al. 2011)[5] is to compare hydrologic projections from both the Hydrologic Modelling and the Regional Climate Modelling Diagnostics projects.

Arelia T. Werner, Hydrologist, PCIC

22 December 2010

[3] Rodenhuis, D., K.E. Bennett, A.T. Werner, T.Q. Murdock and D. Bronaugh, 2009: *Climate overview 2007: Hydro-climatology and future climate impacts in British Columbia*. Pacific Climate Impacts Consortium, University of Victoria, Victoria, BC, 132 pp.
[4] Rodenhuis, D., Braun, M., Music, B., Caya, D, 2011: *Climate diagnostics of future water resources in BC watersheds, Hydrologic Impacts*. Pacific Climate Impacts Consortium, University of Victoria, 74 pp.
[5] Shrestha, R.R., A.J. Berland, M.A. Schnorbus, A.T. Werner, 2011: *Climate change impacts on hydro-climatic regimes in the Peace and Columbia watersheds, British Columbia, Canada*. Pacific Climate Impacts Consortium, University of Victoria, Victoria, BC, 37 pp.

BCSD Downscaled Transient Climate Projections for Eight Select GCMs over British Columbia, Canada

(BLANK)

Executive Summary

Projections of temperature and precipitation were required to drive a macro-scale hydrologic model, the Variable Infiltration Capacity model, to produce future projections of monthly streamflow in three BC watersheds (Columbia, Peace, Campbell) for the 2050s. Global Climate Models (GCMs) commonly operate at too coarse of resolution (~100 km) to be meaningful for assessing local-scale impacts. Statistical downscaling is one approach to translate large-scale information to a local-scale where relationships between large-scale variables in the GCM and local-scale climate variables in the observed record are used to adjust GCM projections to better represent local conditions. Before downscaling, GCMs were screened based on a number of performance metrics including performance over the globe, Northern Hemisphere, North America and western North America. This resulted in the selection of eight GCMs from the 23 available models: CGCM3.1 (T47); CSIRO-Mk3.0; CCSM3; GFDL-CM2.1; MIROC3.2 (medres); ECHAM/MPI-OM; UKMO-HadCM3; and UKMO-HadGEM1. All runs of these selected models under emissions scenarios B1, A1B and A2 were used where available (UKMO-HADGEM1 did not have B1). These models are the same models which have been chosen by similar studies in North America.

The Bias Corrected Spatial Disaggregation (BCSD) statistical downscaling technique was chosen for application in this case due to its extensive use, particularly in previous hydrologic modelling studies. In this approach, the monthly GCM data is bias-corrected against the gridded-observed data at the GCM grid-scale. The bias-corrected results are scaled to match the observed spatial pattern and re-sampled values from the gridded-observed record are adjusted to match the monthly GCM totals. As a result, projections of future precipitation, minimum temperature and maximum temperature at 1/16° were created. This technique was validated by comparing BCSD downscaled NCEP results to gridded-observed data at the 1/16° grid-scale over BC for the validation period (1991-2000). For average temperature, median differences were -0.3°C in July and -0.6°C in December. For precipitation, BCSD downscaled NCEP results produced differences of -4% of gridded-observations based on the median in July and 0% in December. Downscaled NCEP results matched the explained variance of the gridded-observations at the 99% confidence interval for several temperature and precipitation indices.

Based on the median results of 23 climate change scenarios downscaled using BCSD, annual mean temperature is projected to increase by 2.3°C and annual precipitation is projected to increase by 8% on average over BC by the 2050s when compared to 1961-1990. Warming is projected to be greatest in winter and the least in spring and fall. Precipitation is projected to increase most in spring and decrease in summer on average over the province. Annually, the Okanagan, Columbia and Peace Basins are projected to have the greatest temperature increase, while the Northwest and Peace Basin are projected to have the largest precipitation increase. In the winter, the greatest warming is projected for the Peace Basin, while in summer the greatest warming is projected for the Okanagan. In the spring and fall, projected warming is relatively uniform across all regions. Precipitation is projected to increase the most out of any region in the Peace Basin in all seasons, except summer. Decreases are projected during the summer for the South Coast, Okanagan, Columbia, Fraser and North Coast.

To test the benefits of using BCSD to downscale a GCM, BCSD results for CGCM3 A2 were compared to those of the un-corrected CGCM3 A2. The BCSD process was found to improve the ability of the CGCM3 model to represent the variability in precipitation across the province, but altered the temperature projections very little. The contribution to the range of uncertainty of GCMs versus emissions scenarios was investigated by downscaling several GCMs, run under several emissions scenarios. The range between temperature and precipitation projections for the 2050s was greater for the multiple GCMs than it was for emissions scenarios, both annually and seasonally. The range in seasonal response among models was greater than the range in annual response. The BCSD downscaled CGCM3 A2 scenario was the second warmest scenario after HADGEM A2 in winter, the third coolest in spring, summer and fall,

and the wettest (summer) or second wettest model out of the eight models selected for downscaling in all seasons.

Acronyms and Abbreviations

Acronym/Abbreviation	Description
AHCCD	Adjusted Historical Canadian Climate Data (http://www.cccma.ec.gc.ca/hccd/)
ASP	automated snow pillow
AVHRR	Advanced Very High Resolution Radiometer
BCSD	Bias Corrected Spatial Disaggregation
BTM	Baseline Thematic Mapping
CCCma	Canadian Centre for Climate Modelling and Analysis (Victoria, Canada) (http://www.cccma.ec.gc.ca/)
CCSM3.0	Community Climate System Model, version 3.0 (NCAR, US)
CCSR	Center for Climate System Research (University of Tokyo, Tokyo, Japan)
CGCM3.1	Coupled Global Climate Model, version 3.1 (CCCma, Canada)
CGIAR-CSI	Consultative Group on International Agricultural Research – Consortium for Spatial Information (http://csi.cgiar.org/meeting/index.asp)
CIG	Climate Impacts Group (University of Washington, Seattle, USA)
ClimateWNA	Climate Western North America (http://www.genetics.forestry.ubc.ca/cfcg/ClimateWNA/ClimateWNA.html)
CMIP3	Coupled Model Intercomparison Project, phase 3 (http://cmip-pcmdi.llnl.gov/cmip3_overview.html)
CMIP5	Coupled Model Intercomparison Project, phase 5 (http://cmip-pcmdi.llnl.gov/cmip5/index.html)
CSIRO	Commonwealth Scientific and Research Organization (Australia) (http://www.csiro.au/)
DEM	Digital Elevation Model
DSMW	Digital Soil Map of the World
EC	Environment Canada
ECHAM5	European Centre Hamburg Model, version 5 (MPI, Germany)
EOSD	Earth Observation for Sustainable Development
ENSO	El Niño/Southern Oscillation
FAO	Food and Agricultural Organization (http://www.fao.org/)
GCM	global climate model
GFDL	Geophysical Fluid Dynamics Laboratory (http://www.gfdl.noaa.gov/)
GHG	greenhouse gas
HADCM3	Hadley Centre Coupled Model, version 3 (Hadley Centre, UK)
HADGEM1	Hadley Centre Global Environmental Model, version 1 (Hadley Centre, UK)

IPCC	Intergovernmental Panel on Climate Change (http://www.ipcc.ch/)
IQR	inter-quartile range
IRF	instantaneous response function
ISRIC	International Soil Reference and Information Centre (http://www.isric.org/)
LOESS	locally weighted regression
MCPI	Model Climate Performance Index
MIROC	Model for Interdisciplinary Research on Climate (CCSR, Japan)
MOCOM	Multi-Objective Complex Evolution Method
MPI	Max Planck Institute (http://www.mpg.de/english/portal/index.html)
MVI	Model Variability Index
NARCCAP	North American Regional Climate Change Assessment Program (http://www.narccap.ucar.edu/)
NARR	North American Regional Reanalysis
NCAR	National Center for Atmospheric Research (http://ncar.ucar.edu/)
NCEP	National Centers for Environmental Prediction (http://www.ncep.noaa.gov/)
PCMDI	Program for Climate Model Diagnosis and Intercomparison (http://www-pcmdi.llnl.gov/)
POI	point of interest
PDO	Pacific Decadal Oscillation
PRISM	Parameter-elevation Regressions on Independent Slopes Model
RCM	regional climate model
RCP	Representative Concentration Pathways
SOM	self-organizing maps
SLP	sea level pressure
SPOT-4	Satellite Pour l'Observation de la Terre, satellite 4
SRES	Special Report on Emission Scenarios
SRTM	Shuttle Radar Topography Mission
SVATS	soil-vegetation-atmosphere transfer scheme
SWE	snow water equivalent
UKMO	United Kingdom Meteorological Office (http://www.metoffice.gov.uk/)
UNESCO	United Nations Educational, Scientific and Cultural Organization (http://www.unesco.org/new/en/unesco/)
USHCN	United States Historical Climatology Network (http://cdiac.ornl.gov/epubs/ndp/ushcn/ushcn.html)
VIC	Variable Infiltration Capacity model (http://www.hydro.washington.edu/Lettenmaier/Models/VIC/)

WCRP   World Climate Research Program (http://www.wcrp-climate.org/)

WSC   Water Survey of Canada (http://www.ec.gc.ca/rhc-wsc/)

(BLANK)

1. Introduction and Background

Global climate change due to anthropogenic greenhouse gas emissions will influence climate conditions in British Columbia. Expected warming and changing precipitation patterns are anticipated to have a large effect on the hydrology of western North America, with significant implications for water resources and the economy, infrastructure, and ecosystems. The hydrologic response to climate change may potentially impact many water-dependent resources and activities, including hydroelectric generation, municipal water supply, flood management, in-stream flow needs and fish habitat, irrigated agriculture, recreation and navigation. Naturally, as all these issues are relevant within BC, the degree to which local and regional hydro-climatology may be susceptible to the impacts of climate change is of considerable concern. Although climate change is taking place on a global scale, understanding the impacts of continued warming and changing of precipitation patterns on local- and regional-scale hydrology is most relevant to water resources planning and adaptation.

Hydrologic projections require climate projections that are derived from global climate models (GCMs), the only tools we have available to us to explore the response of the global climate system to scenarios of future greenhouse gas emissions. GCMs provide a representation of the earth's climate system based on first principles. They simulate differing responses to similar greenhouse gas forcing due to differences in implementation and the effects of natural internal low-frequency variability in the climate system. All of these models represent the inherent stochastic nature of the earth's climate system. As a result, projections may not agree over the globe and can differ strongly, especially in smaller regions. GCMs are run at relatively coarse resolutions with grid spacing of a 100 km or more. Within BC, the regional climate response will be affected by large topographic relief, strong precipitation gradients and continentality. Statistical downscaling is an approach often adopted to translate large-scale information to a local scale, where relationships between large-scale variables in the GCM and local-scale climate variables in the observed record are used to adjust GCM projections to better represent local conditions. The statistical downscaling technique applied here, Bias Corrected Spatial Disaggregation (BCSD), both bias corrects and spatially disaggregates the raw monthly GCM output to provide more local and regional detail on potential climate change effects at the daily time step.

As a requirement to provide driving data at the daily time step for hydrologic modelling, climate projections have been generated for the province as a whole at a spatial resolution of 1/16°. The climate projections have been produced from a suite of eight latest-generation global climate models driven by three emissions scenarios, including projections for the 2050s that range from a future with relatively less warming and more moistening ("cool/wet") to relatively more warming and less moistening ("warm/dry"). This ensemble approach explicitly addresses both emissions and GCM uncertainty in the final projections. Although originally developed to provide the boundary conditions for hydrologic modelling, the spatial scope and detail of the resulting downscaled projections affords a unique opportunity to more generally assess and quantify the regional variation in projected temperature and precipitation trends in BC.

This work also expands upon climate change projections originally produced by PCIC in the *Climate Overview 2007* report (Rodenhuis et al. 2009). In Rodenhuis et al. (2009), GCMs were described and future projections for 15 of the 22 available models over BC were outlined. This was done in the native resolution of the models (~100 km). The current work will present a case for selecting a sub-set of those 15 GCMs based on their performance historically in the region, compare the 1/16° (~6 km grids) BCSD results to those lower-resolution results presented in the *Climate Overview*, and discuss similarities in the range of uncertainty resulting from models versus emissions scenarios for the two approaches.

The remainder of this report is organized into six sections that provide, respectively: 1) methods, including GCM selection and statistical downscaling, 2) validation of the statistical downscaling procedure for BC, 3) results and discussion of regional precipitation and temperature changes, 4) a discussion of uncertainty, 5) conclusions and 6) future work. Figures are included with the text and

captions are numbered by section. All references plus figure and table listings are located at the end of the report.

2. Methods

2.1 Climate Projections

The climate models of today rest on principles developed in the mid-20th century when efforts were primarily focused on representing the current climate, starting with numerical weather prediction models in the 1950s. The first models, which simulated atmospheres that resembled observations, were developed in 1965. At that time, those working on the problem concluded that in order to move forward they would need computers that were much more powerful than those that were available. Over time, computing power increased and ocean circulation became a part of models in the early 1980s, allowing the modelled ocean to exchange heat with the atmosphere. By 1988, modellers felt they had a basic grasp of the main forces and variations in the atmosphere and interest shifted from perfecting the representation of current climate to studying long-term climate and representing the "transient response" to changes in conditions (Weart 2008). Computing power was sufficient to allow modelling groups to confidently explore climate through time.

In the 21st century we simulate the atmosphere with numerical models. As these developed from weather models they were first known as General Circulation Models that represent the physical processes in the atmosphere, ocean, cryosphere and land surface. Early in the 21st century General Circulation Models became known as Global Climate Models because they had started to incorporate much more than the circulation of the atmosphere as vegetation, ocean chemistry, ice sheets, and ecosystems were represented in the new suite of models (Weart 2008). As per the Intergovernmental Panel on Climate Change:

 "GCMs depict the climate using a three dimensional grid over the globe, typically having a horizontal resolution of between 250 and 600 km, 10 to 20 vertical layers in the atmosphere and sometimes as many as 30 layers in the oceans." (IPCC 2008)

Those processes which occur at scales smaller than several hundred kilometers cannot be modelled at this scale and therefore their known properties must be represented with averages over the large-scale. For example, clouds must be addressed in this way. This is known as parameterization and is one source of uncertainty in GCM-based simulations of future climate. Feedback mechanisms such as water vapour and warming, clouds and radiation, ocean circulation and ice and snow albedo also must be parameterized. The way these processes are modelled differs from one group to another and results in different models having different responses to the same greenhouse gas forcing (IPCC 2008).

The state of the art models of today include interactive clouds, oceans, land surface and aerosols. Some models also include detailed chemistry and the carbon cycle. These components are considered important for several reasons (Pope 2007):

- Clouds impact how much radiation from the sun reaches the earth's surface and how much warmth is trapped near the surface at night. There are many types of clouds and each has a different effect on the climate.
- Oceans warm more slowly than land and they transport heat around the globe via ocean currents.
- Land surface cover, such as trees or crops, impacts the albedo, or the amount of radiation reflected or absorbed by the earth's surface. Darker areas absorb radiation and light areas, such as those covered in snow or ice, reflect it.
- Aerosols are particles in the atmosphere that are produced naturally from volcanoes and forest fires and when fossil fuels are burned. Generally, aerosols have a cooling effect on climate by reducing the amount of sunlight reaching the surface and they change the properties of clouds, but their impact is relatively short-term.

- The amount of carbon dioxide that remains in the atmosphere depends on how much is taken up by the biosphere (plants, soils, phytoplankton) and some of these, such as soils, might not be able to take up CO_2 under increased temperatures.

It should be noted that Coupled Model Inter-comparison Project phase 3 (CMIP3) class models generally do not have land ice sheets nor do they represent the carbon cycle.

Work developing GCMs in the last decade led the Intergovernmental Panel on Climate Change (IPCC) to conclude that human influence on climate had most likely been detected (IPCC 2007a). This is because the pattern of atmospheric heating that GCMs computed when increased greenhouse gases were included was different from the pattern of other influences alone and models forced with increased greenhouse gases produced climates most similar to the observed record of climate change. Earlier, analysis of ice core records had provided an independent estimate of the amount of warming resulting from increasing CO_2, otherwise known as the climate's sensitivity. It showed roughly two degrees of warming for doubled CO_2, which reinforced the findings of GCMs. However, this is only some of the evidence in support of recent climate change being a result of anthropogenic activities. Much more on this topic can be found in Hegerl et al. (2007).

Uncertainty is an inherent aspect of climate projections. There are several steps in the modelling process that add uncertainty. Projections of future emissions trajectories hold some of the largest uncertainty over longer time horizons (i.e., out to 2100). For the 2050s period, climate projections obtained under three different emissions trajectories (A1B, A2 and B1) are relatively indistinguishable and the range in response is attributable to different models (Bennett et al. 2009). Specifically, projection uncertainty stems from boundary conditions (e.g., greenhouse gas concentrations and radiative forcing), structural uncertainty (e.g., which processes are included, which processes are excluded, and how small-scale phenomena are parameterized), model numerics (temporal and spatial resolution, type of grid, numerical algorithms, etc.), parameter uncertainty, and to a lesser degree, errors and uncertainty in initial conditions (Tebaldi and Knutti 2007). On smaller spatial scales and shorter time horizons, initial conditions can become the more dominate source of uncertainty over others mentioned above (Hawkins and Sutton 2009). Uncertainty in observational data also makes it difficult to assess the strengths and weaknesses of the available models. To explore a large portion of the emissions and GCM uncertainty we have selected multiple GCMs following three emissions scenarios that cover a large range in wet/dry and warm/cool combinations using a single result (run 1) from an ensemble of different GCMs.

2.2 GCM Selection

Seventeen modelling centers participated in modelling future climate for the Intergovernmental Panel on Climate Change (IPCC) Fourth Assessment Report (AR4; Meehl et al. 2007). At some centers, more than one model was applied as the centers tried different resolutions or parameterizations of the same model (Table 2-1). Data from 25 GCMs have been collected in the CMIP3, which is archived at the Program for Climate Model Diagnosis and Inter-comparison at Lawrence Livermore National Laboratory (LLNL) making the data publicly accessible (PCMDI 2010). It is the recommendation of the IPCC that all available models should be used for climate change studies as no one model has been identified as more robust (Randall et al. 2007). That being said, some models probably can be excluded and/or need to be excluded to make the ensemble number manageable for users. With multiple models being run multiple times under multiple emissions scenarios, there are upwards of ~144 available scenarios, making it unreasonable for researchers to incorporate all available scenarios into their analysis. Translating coarse-scale data to the local-scale requires statistical downscaling that is computationally demanding to complete for all available GCMs. Furthermore, some models appear to not be representative at regional scales when compared over the historical record to gridded-observational data, although they may have performed well globally (Overland and Wang 2007). Faced with these challenges, some studies

conducted at the regional scale have selected a sub-set of models from the CMIP3 suite to avoid outliers and reduce the range in possible futures based on the performance of GCMs when compared to observed historical data (e.g., Overland and Wang 2007; Hamlet et al. 2010). Under these tests, model ranking depends on the metric used, and when several credibility measures are combined, the overall tendency is for models to perform comparably (Brekke et al. 2006). It should be noted that a model's skill in reproducing historical climate normals speaks somewhat to its reliability in a given region, but does not reflect how a given model will respond to future greenhouse gas forcing (Hamlet et al. 2010). Response of a given model to a greenhouse gas forcing is referred to as its sensitivity, which differs between models and is usually measured in terms of change in temperature resulting from a given increase in carbon dioxide. A universal set of performance metrics has not been established (Gleckler et al. 2008). Instead researchers are encouraged to outline their rationale to allow for reproducibility (Tebaldi, pers comm.). The following outlines the rationale applied for this study.

Various studies have shown that a multi-model average yields better prediction and compares more favorably to observations than any single model when compared over multiple variables (Knutti et al. 2010). The multi-model average tends to be an improvement over individual models because the bias in one model is cancelled out by another. Incorporating information from different models contributes to the increase in skill as each model has different strengths in representing different facets of the climate (Pierce et al. 2009). Yet bias cannot be completely removed, even when all models are included. The amount of bias that can be removed on average over the globe for randomly selected models is significantly reduced after including five models and levels off after 10 (Knutti et al. 2010). When the "best" performing models are analyzed in the same way, the RMS bias removed matches or exceeds that for randomly selected models after six or eight models, depending on the season. This has been reaffirmed by others working in the western US, who have found that model skill asymptotes after including approximately five different models (Pierce et al. 2009), and also in BC in a yet unpublished study by Valentina Radic. Thus, an average from five to eight "best" performing models should be most comparable with observations and avoids processing of all available GCMs while removing a similar amount of bias.

Averaging can be based on "one model, one vote" or can be weighted, based on past relationships between forecasts and verifications using Bayesian methods, although defining a robust weighting system is difficult (Pierce et al. 2009; Knutti et al. 2010). Therefore, models will be screened based on their historical performance, eliminating those which do not pass our criteria and giving those which remain equal weighting. The statistical paradigm that informs our interpretation of the final climate projection ensemble can be formally classified as "indistinguishable-weighted" (Tebaldi, pers. comm.). It has been argued that the reliability of model projections may be improved if GCM results are weighted according to some measure of skill (i.e., GCM results are not treated equally; Amman and Hargreaves 2010; Knutti et al. 2010; Tebaldi and Knutti 2007). Furthermore, climate projections from the final ensemble of selected GCM-scenario pairs are treated as statistically indistinguishable and given equal weight (Annan and Hargreaves 2010 and Knutti et al. 2010). In such a case, it is taken that "the truth is drawn from the same distribution as the ensemble members, and thus no statistical test can reliably distinguish one from the other" (Annan and Hargreaves 2010). Each ensemble member is considered indistinguishable from all possible outcomes of the earth's chaotic processes (Knutti et al. 2010). This concept has also been described as "exchangeability" (Rougier et al. 2010). In the following section, we evaluate the performance of 22 available GCMs from CMIP3 using a variety of performance metrics based on work by extramural groups (e.g., Gleckler et al. 2008; Pincus et al. 2008; Pierce et al. 2009; Moore et al. 2010). Models are screened according to their performance on both the global and regional scales, and although temperature and precipitation will be the only variables used from the GCMs, they are screened for several variables. This is because models are thought to be more easily adjustable to match historical temperature and precipitation than other variables. Therefore, representation of other variables was taken as a demonstration of how well the model is able to represent the climate as a whole.

Table 2-1. Model identification, originating group, and atmospheric resolution.

IPCC ID	Centre and Location	Atmospheric Resolution
BCCR-BCM2.0	Bjerknes Centre for Climate Research (Norway)	T63 L31
CGCM3.1(T47)	Canadian Centre for Climate Modelling and Analysis (Canada)	T47 L31
CGCM3.1(T63)		T63 L31
CSIRO-Mk3.0	CSIRO Atmospheric Research (Australia)	T63 L18
CNRM-CM3	Meteo-France, Centre National de Recherches Meteorologiques (France)	T42 L45
ECHO-G	Meteorological Institute of the University of Bonn, Meteorological Research Institute of KMA, and Model and Data group (Germany and Korea)	T30 L19
GFDL-CM2.0	US Dept. of Commerce, NOAA Geophysical Fluid Dynamics Laboratory (USA)	N45 L24
GFDL-CM2.1		N45 L24
GISS-AOM		90 x 60 L12
GISS-EH	NASA/Goddard Institute for Space Studies (USA)	72 x 46 L17
GISS-ER		72 x 46 L17
FGOALS-g1.0	LASG/Institute of Atmospheric Physics (China)	128 x 60 L26
INM-CM3.0	Institute for Numerical Mathematics (Russia)	72 x 45 L21
IPSL-CM4	Institut Pierre Simon Laplace (France)	96 x 72 L19
MIROC3.2(medres)	Center for Climate System Research (The University of Tokyo), National Institute for Environmental Studies, and Frontier Research Center for Global Change (JAMSTEC) (Japan)	T42 L20
MIROC3.2(hires)		T106 L56
MRI-CGCM2.3.2	Meteorological Research Institute (Japan)	T42 L30
ECHAM5/MPI-OM	Max Planck Institute for Meteorology (Germany)	T63 L32
CCSM3	National Center for Atmospheric Research (USA)	T85 L26
PCM		T42 L18
UKMO-HadCM3	Hadley Centre for Climate Prediction and Research Met Office (UK)	96 x 72 L19
UKMO-HadGEM1		N96 L38

*T#/N#/# x # refer to the spatial resolution of the surface grid, L# refers to the number of vertical levels

Models are screened on the global-scale based on results from Gleckler et al. (2008). As GCMs are designed to replicate the global climate system, poor performance of the model over the historical period was assumed to indicate problems that might lead to erroneous results on the regional-scale. At the global scale, models were evaluated based on their relative errors. The relative error is defined, for a given model and a given climate field, as the root mean square (RMS) error between a simulated field and a corresponding reference dataset (observations) subtracted by the 'typical' model error, all divided by the 'typical' error. The 'typical' error is defined as the median of the RMS error calculations. The relative error is a measure of how well a given model (with respect to a particular dataset) compares with the typical model error. For example, if the relative error has a value of -0.2, then the model's RMS error is 20% smaller than the 'typical' model. Observational datasets differed by variable, but were primarily sourced from re-analysis (ERA40, European Centre for Medium-Range Weather Forecasts and NCEP/NCAR, National Centers for Environmental Prediction-National Center for Atmospheric Research, or Earth Radiation Budget Experiment (ERBE)/Clouds and the Earth's Radiant Energy System (CERES) datasets (Gleckler et al. 2008). For monthly mean climatological data such as temperature, total precipitation, and geopotential height, the RMS error statistic accounts for errors in both the spatial pattern and the annual cycle. Gleckler et al. (2008) calculated relative errors for all 22 GCMs from CMIP3 and 26 climate fields over 1980-1999. Models whose relative error was 0.5 or greater for any variable were considered to perform poorly over the globe.

To assess models at the more regional scale, we referred to work completed by Radic (in Moore et al. 2010) who evaluated all 22 CMIP3 GCMs at the regional (North America) and sub-regional (western

North America) scale. The North American Regional Reanalysis (NARR) data (~32 km) formed the basis for comparison, but was interpolated to 10XNARR resolution (~320 km) to be more comparable to GCM resolution (~100 km). Climate fields from all 22 GCMs were interpolated to 10xNARR resolution and compared to NARR over 1980-1999. Model performance was analyzed on two spatial domains: 'large' domain, equivalent to the original NARR domain, and 'small' domain that roughly covers the NW corner of the 'large' domain. Relative model errors, variance ratios, and model performance indexes for these two domains and several climate fields of interest, including temperature and specific humidity at 850 hPa, geopotential height at 500 hPa and 850 hPa, sea level pressure and precipitation, were calculated. Two model performance indexes were adapted from Gleckler et al. (2008) and applied over these regional domains: the 'Model Climate Performance Index' (MCPI) and the 'Model Variability Index' (MVI). With the MCPI each model's relative error was averaged across the climate fields of interest. Model simulation of inter-annual variability was examined against variances of monthly mean anomalies, computed relative to the monthly climatology for the period 1980-1999 with the MVI. For each GCM and climate field of interest, smaller values indicated better agreement with the reference data. Models in the bottom place according to Radic's (in Moore et al. 2010) set of statistical metrics (relative error, MCPI and MVI) for any climate variable and spatial domain were considered to have poor performance regionally.

Radic (in Moore et al. 2010) also analyzed GCMs using Self-Organizing Maps (SOMs) for Sea Level Pressure (SLP) to test the GCMs' replication of synoptic patterns present in NARR. An SOM is a type of unsupervised Artificial Neural Network suited to pattern recognition and classification, similar to cluster analysis. In Radic's (2010) analysis, the input data consisted of daily SLP anomalies from NARR for each of the 21 available GCMs (data for HADGEM1 was not available). SOM training was applied on a seasonal basis, producing SLP anomaly (Pa) patterns that are characteristic for each season (DJF, MAM, JJA, SON) and was performed independently for the 'large' and 'small' spatial domains. Different SOM sizes were chosen, which provided reasonable compromises between detail and interpretability. The size or number of nodes of the SOM reflects the number of classes to which the patterns are binned. Based on the sizes 4x3, 4x4 and 5x4 the number of classes defined were 12, 16 and 20, respectively. Ideally, a model would recreate the same synoptic patterns that are seen in the real atmosphere, here represented by NARR, and would have the same frequency of occurrences for each of the SOM nodes. Models that did not have a significant correlation between their node frequencies and those from NARR for at least one season, over both the 'large' and 'small' domain, and all SOM sizes were given a low rank.

Results from the studies described above were used to guide the GCM selection. Table 2-2 provides a summary of how each model performed under seven decision factors. To make the evaluation consistent, only the first run for GCMs that have multiple runs for each climate scenario were evaluated. Ideally, enough model realizations must be chosen to account for the effects of natural internal variability within a model (Pierce et al. 2009). However, multiple realizations are not equally available from all centers, and resources to work with these vast datasets were limited. Additionally, a collection of models from multiple centers will sample both internal variability and structural differences provided it includes a sufficient number of models.

Table 2-2. Selection of GCMs

	GCM	Decision Factors						
		1	2	3	4	5	6	7
1	BCCR-BCM2.0	A			A	A	A	
2	**CGCM3.1(T47)***	A	A	A	A	A	A	A
3	CGCM3.1(T63)	A	A	A	A	A		
4	**CSIRO-Mk3.0***	A	A	A	A	A	A	
5	CNRM-CM3	A			A	A	A	
6	ECHO-G		A		A	A	A	
7	GFDL-CM2.0	A	A		A	A	A	A
8	**GFDL-CM2.1***	A	A	A	A	A	A	A
9	GISS-AOM	A			A			
10	GISS-EH	A						
11	GISS-ER	A	A			A	A	
12	FGOALS-g1.0	A						
13	INM-CM3.0	A				A	A	
14	IPSL-CM4	A					A	
15	**MIROC3.2(medres)***	A		A	A	A	A	
16	MIROC3.2(hires)	A	A	A	A	A		
17	MRI-CGCM2.3.2	A				A	A	
18	**ECHAM/MPI-OM***	A	A	A	A	A	A	
19	**CCSM3**	A	A	A			A	A
20	PCM	A						
21	**UKMO-HadCM3***	A	A	A	A	A	A	A
22	**UKMO-HadGEM1**		A	A		^		

1) Monthly GCM data for 20th and 21st century were fully accessible for the model (archived at the LLNL).
2) Model's relative error for 1980-1999 annual cycle climatology calculated in *Gleckler et al.* (2008) was not greater than 0.5 for any considered climate variable over the full global domain. In other words, models with relative errors larger than 50% from the 'typical' error (median of relative errors across the 22 GCMs) were excluded from the ensemble.
3) Model was in the top 10 according to the MCPI over the Northern Hemisphere in *Gleckler et al.* (2008).
4) When ranked according to *Radic's* (in *Moore et al.,* 2010) set of statistical metrics (relative error, MCPI and MVI) the model was not in the bottom place for any climate variable and spatial domain.
5) According to GCM evaluation with SOM, the model produced node frequencies that were significantly correlated to node frequencies from NARR for at least one season, over both 'large' and 'small' domain, and all SOM sizes. In other words, models with no significant correlation for any season were excluded from the ensemble
6) Model had been used for the Climate Overview (*Rodenhuis, et al.* 2007).
7) Model was part of the North American Regional Climate Change Assessment Program (NACCAAP).

^ Not accessible for UKMO-HadGEM1. Red = 7/7; Burgundy = 6/7; Grey = 5/7; Black < 5/7. Bold and * = Selected.

CGCM3.1(T47), GFDL-CM2.1 and UKMO-HadCM3 were selected as they passed on all factors (Table 2-2). Others met several of the criteria, but not all. To fill out our selection to a total of five to seven models to remove the most amount of bias, four other models were selected. CSIRO-Mk3.0 and ECHAM/MPI-OM were included because they passed on six out of seven decision factors. Both are strong models according to the performance metrics we screened the models against. The only factor they did not meet was being included in NARCCAP, decision factor 7. MIROC3.2(medres) was included because it passed on five out of seven decision factors, performing well over the globe and locally, except for temperature at 200 hPa where its relative error for 1980-1999 annual cycle climatology calculated in Gleckler et al. (2008) was greater than 0.5 over the full global domain. CCSM3 was included because it passed on five out of seven decision factors, including being part of NARCCAP, although it did fail to pass the screening criteria at the regional scale (decision factors 4 and 5). Regionally, CCSM3 ranked between 11th and 20th for the large and small domain for all variables, so overall it was not a very strong model based on work by Radic (in Moore et al. 2010). However, it had been used by several other groups such as NARCAAP and Hamlet et al. (2010) and performed well over the globe (Gleckler et al. 2008). The UKMO-HadGEM1 model was chosen, even though it met less than five out of seven factors because it has been used for other studies (Murdock and Flower 2009; Nelson 2010; Flower et al., submitted). Additionally, UKMO-HadGEM1 was in the bottom place only for precipitation over North America, for all other variables it was ranked in the top five over the large and small domain, including MCPI and MVI based on Radic (in Moore et al. 2010) and had the lowest relative error after the multi-model ensemble over the Northern Hemisphere (Gleckler et al. 2008). Where fewer than six decision factors were met models were generally not selected.

When more than one model from the same modelling centre performed well according to the screening criteria we chose one model to avoid oversampling from the same model population to reduce artificial coherencies between models that might contaminate the statistics in the ensemble (Leduc and Laprise 2010). The model was selected based on which was the stronger of the two as judged by its performance globally and regionally, or if it had been used by other studies in the region. The following centers contributed more than one model: the Canadian Centre for Climate Modelling and Analysis, Canada (CGCM3.1(T47) and CGCM3.1(T63)); US Department of Commerce, NOAA Geophysical Fluid Dynamics Laboratory, USA (GFDL-CM2.0 and GFDL-CM2.1); the NASA/Goddard Institute for Space Studies, USA (GISS-AOM, GISS-EH and GISS-ER); Centre for Climate System Research (The University of Tokyo), National Institute for Environmental Studies, and Frontier Research Center for Global Change, Japan (MIROC(hires/T106) and MIROC(medres/T42)) and the Hadley Centre for Climate Prediction and Research, Met Office, UK (HadCM3 - HadGEM1). CGCM3 T47 - CGCM3 T63 and GFDL CM2.0 - GFDL CM2.1 were found to be similar to each other when compared to the distribution of the root-square differences for all random pairs, especially over western North America (Leduc and Laprise 2010) and are likely redundant when applied in the same study. The GISS models did not meet more than five out of the seven decision factors and thus were not selected for this study. MIROC(hires/T106) - MIROC(medres/T42) and HadCM3 - HadGEM1 diverged over western North America, so applying more than one to the study might have merit (Leduc and Laprise 2010). MIROC(medres/T42) was chosen here over MIROC(hires/T106) because it was shown to be a strong model in other studies (Walsh et al. 2008) and was selected as one of the 15 selected models in the Climate Overview report (Rodenhuis et al. 2009). HadCM3 and HadGEM1 were included in our selection because they were divergent and both had been used for several studies across North America (Bonsal et al. 2003; Murdock and Flower 2009; Hamlet et al. 2010; Nelson 2010; Flower et al., submitted).

The final ensemble consisted of the following eight models and emissions scenarios, listed alphabetically:

Global Climate Model	Emissions Scenarios
1. CGCM3.1(T47)	B1, A1B, A2
2. CSIRO-Mk3.0	B1, A1B, A2
3. CCSM3	B1, A1B, A2
4. GFDL-CM2.1	B1, A1B, A2
5. MIROC3.2(medres)	B1, A1B, A2
6. ECHAM/MPI-OM	B1, A1B, A2
7. UKMO-HadCM3	B1, A1B, A2
8. UKMO-HadGEM1	A1B, A2

2.2.1 Comparison of Selected Models Versus Full Ensemble by Region

Our aim is to use the 21st century climate projections from these eight models, run under atmospheric greenhouse gas concentrations from three SRES scenarios to sample the uncertainty in future projections due to emissions scenarios (A2, A1B, and B1) parameterization and initial conditions (IPCC 2007b). Projections from these models will vary by region. Therefore, the selected models are identified for the three basins of interest in BC (Figure 2-1) in scatter plots of temperature vs. precipitation change in the 2050s (2041-2070) as a difference from 1961-1990 to demonstrate the range of selected models versus the full suite (Figure 2-2, Figure 2-3 and Figure 2-4). The median values of the selected and full suite are shown for the temperature and precipitation changes in each case. Basins investigated were the Campbell (a 1,200 km^2 basin in coastal BC on Vancouver Island), the Peace (a 101,000 km^2 basin in north-eastern BC), and the Columbia (a 104,000 km^2 basin in south-eastern BC), which drains to the US. The range in projected temperature or precipitation change varies by basin. The greatest increases in temperature and precipitation are projected for the Peace Basin in winter and summer (Figure 2-3). Temperatures are

projected to increase while precipitation is projected to decrease in summer for the Campbell Basin (Figure 2-2).

To explore the impact of picking eight GCMs from the 22 available, the mean, median, minimum and maximum values of the full ensemble and the selected subset are presented in Table 2-3. Since the HADGEM1 model met only two of the seven decision factors, results are shown for the ensemble both with and without this model. In all three basins, the median projected temperature and precipitation change in the 2050s of the selected models is similar to the median for all available models. The range of the selected models is narrower than all available models in all seasons, which reflects how the minimum projected temperature increase is greater or the maximum projected temperature of the selected models is less than that of all available models. An exception is summer and fall when maximum projected temperature increase in the selected GCMs equals that for all available GCMs. The median projected temperature increase of the selection that includes HADGEM1 tends to be warmer than the selection that does not in summer and fall, but tends to be cooler in winter and spring for most of the basins. In the winter and spring, the range of projected changes in precipitation of the selected models is narrower than that of all available models, but is almost equivalent in summer and fall. The median projected precipitation changes of the selected models are within a few percent of those for all available models. Including or not including HADGEM1 in the ensemble has minimal effect on precipitation projections in any of the seasons for any of the basins.
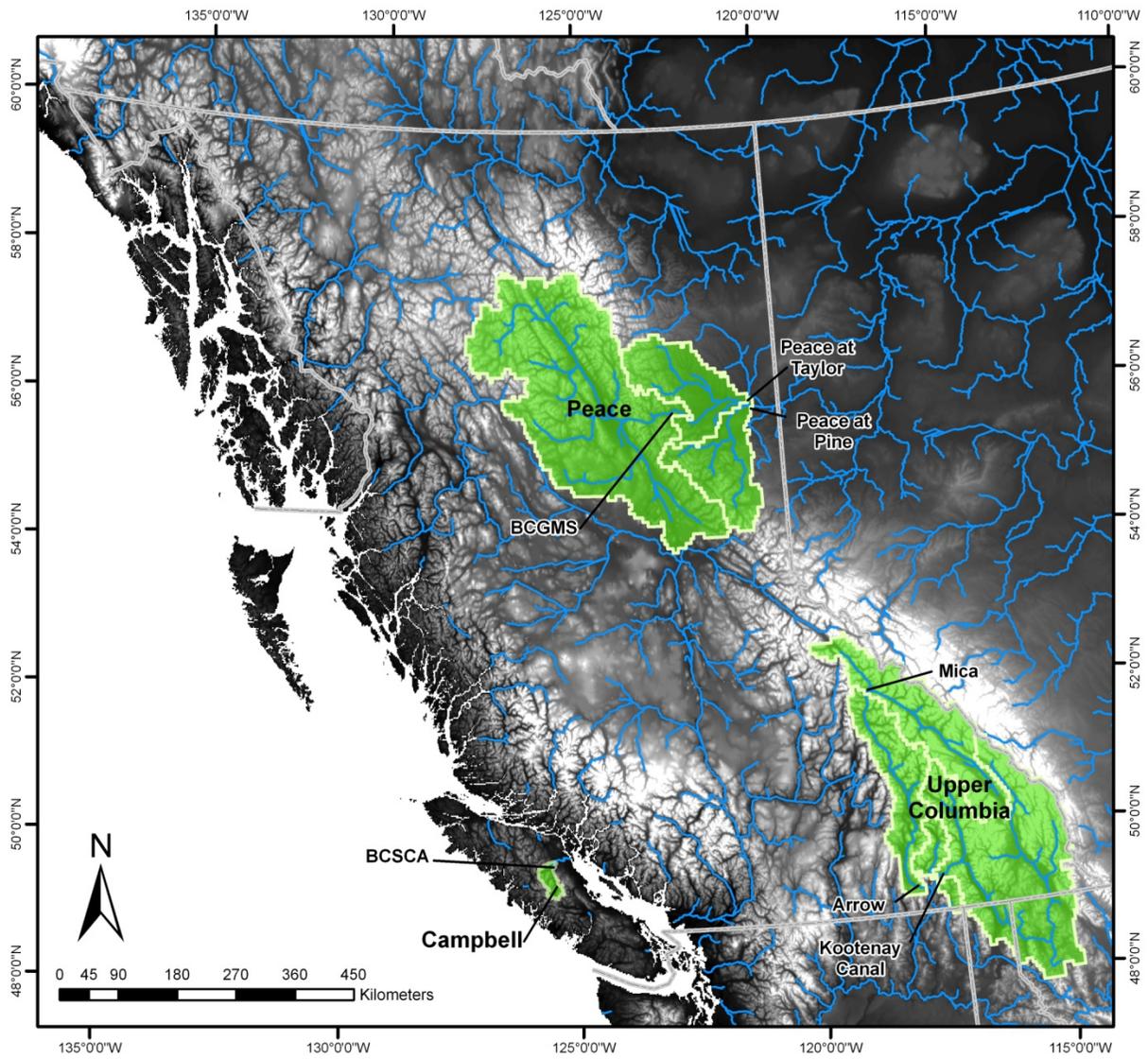
Figure 2-1. Study areas of the hydrologic modelling project.

Table 2-3. Projected changes in temperature for the 2050s versus 1961-1990 by season for the Campbell, Peace and Columbia for all available scenarios (All), the 23 selected scenarios (Sel 1) and for the 21 selected scenarios when UKMO_HadGEM1 is excluded from the selection (Sel 2).

		Temperature											
		Winter			Spring			Summer			Fall		
		All	Sel 1	Sel 2	All	Sel 1	Sel 2	All	Sel 1	Sel 2	All	Sel 1	Sel 2
Campbell	Min	0.3	0.7	0.9	0.4	0.7	0.7	0.9	1.2	1.2	0.4	1.3	1.3
	Max	4.9	2.9	2.9	4.6	4.1	4.1	4.7	4.7	4.7	3.5	3.5	3.5
	Mean	1.9	1.9	2.0	1.7	1.9	1.9	2.2	2.5	2.4	1.9	2.1	2.0
	Med	1.9	2.0	2.1	1.6	1.8	1.7	2.2	2.4	2.2	1.8	2.0	1.8
Peace	Min	0.2	0.5	1.6	0.4	1.0	1.0	0.8	1.2	1.2	0.4	1.2	1.2
	Max	5.7	4.1	4.1	4.6	3.0	3.0	4.0	4.0	4.0	3.9	3.9	3.9
	Mean	2.7	2.7	3.0	1.9	1.9	2.0	2.0	2.3	2.2	2.0	2.2	2.2
	Med	2.6	2.8	3.2	1.9	1.9	2.0	1.9	2.1	2.0	2.0	2.1	2.1
Columbia	Min	0.2	1.2	1.2	0.4	0.9	0.9	1.1	1.3	1.3	0.6	1.4	1.4
	Max	4.4	3.6	3.6	4.2	3.3	3.3	5.0	5.0	5.0	3.9	3.9	3.9
	Mean	2.3	2.3	2.4	1.9	2.0	2.0	2.6	3.0	2.8	2.1	2.3	2.3
	Med	2.1	2.2	2.2	1.8	1.8	2.0	2.4	2.9	2.6	2.0	2.4	2.1

Table 2-4. Projected changes in precipitation for the 2050s versus 1961-1990 by season for the Campbell, Peace and Columbia for all available scenarios (All), the 23 selected scenarios (Sel 1) and for the 21 selected scenarios when UKMO_HadGEM1 is excluded from the selection (Sel 2).

		Precipitation											
		Winter			Spring			Summer			Fall		
		All	Sel 1	Sel 2	All	Sel 1	Sel 2	All	Sel 1	Sel 2	All	Sel 1	Sel 2
Campbell	Min	-10	-8	-8	-10	-4	-2	-44	-44	-44	-8	-8	-2
	Max	26	13	13	25	25	25	13	12	12	23	21	21
	Mean	6	5	5	7	8	9	-15	-16	-13	8	7	9
	Med	6	4	5	6	7	8	-15	-14	-12	10	7	8
Peace	Min	-9	6	6	-1	-1	-1	-18	-18	-18	-3	-2	-2
	Max	26	26	23	31	22	22	19	13	13	25	24	24
	Mean	11	14	13	11	13	13	1	1	1	11	11	11
	Med	11	13	12	10	14	14	1	3	3	11	10	12
Columbia	Min	-8	-1	-1	-4	-4	-4	-27	-27	-27	-5	-5	-5
	Max	24	20	18	24	22	22	13	13	13	20	20	20
	Mean	8	9	8	10	12	13	-8	-8	-7	7	8	9
	Med	10	10	6	9	12	12	-7	-7	-5	7	8	9
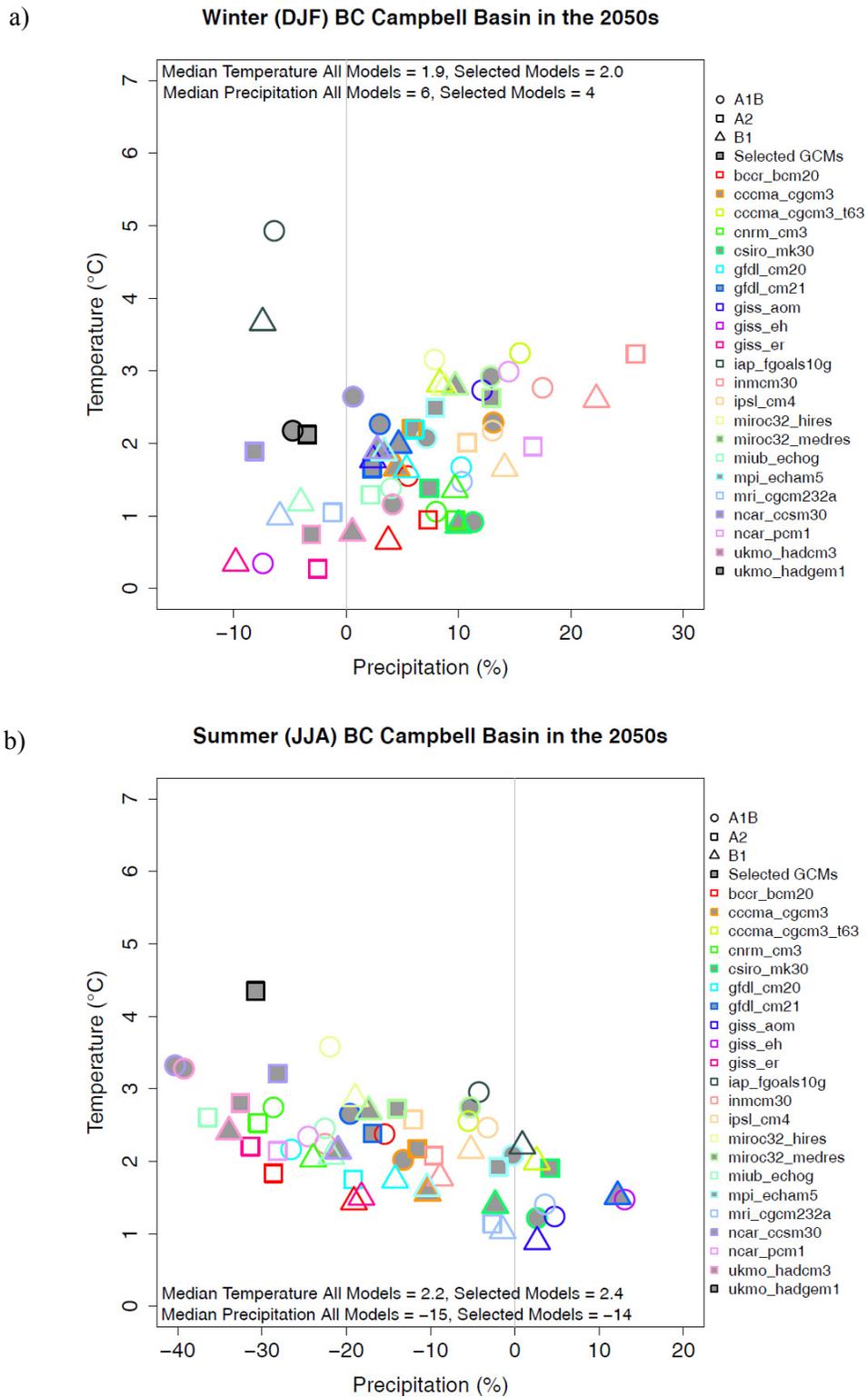
Figure 2-2. Projected temperature (°C) and precipitation (%) in the 2050s in winter (a) and summer (b) as a difference from 1961-1990 in the Campbell Basin based on GCM output. Selected models are shown with grey infilling.

a)

Winter (DJF) BC Peace Basin in the 2050s

b)

Summer (JJA) BC Peace Basin in the 2050s
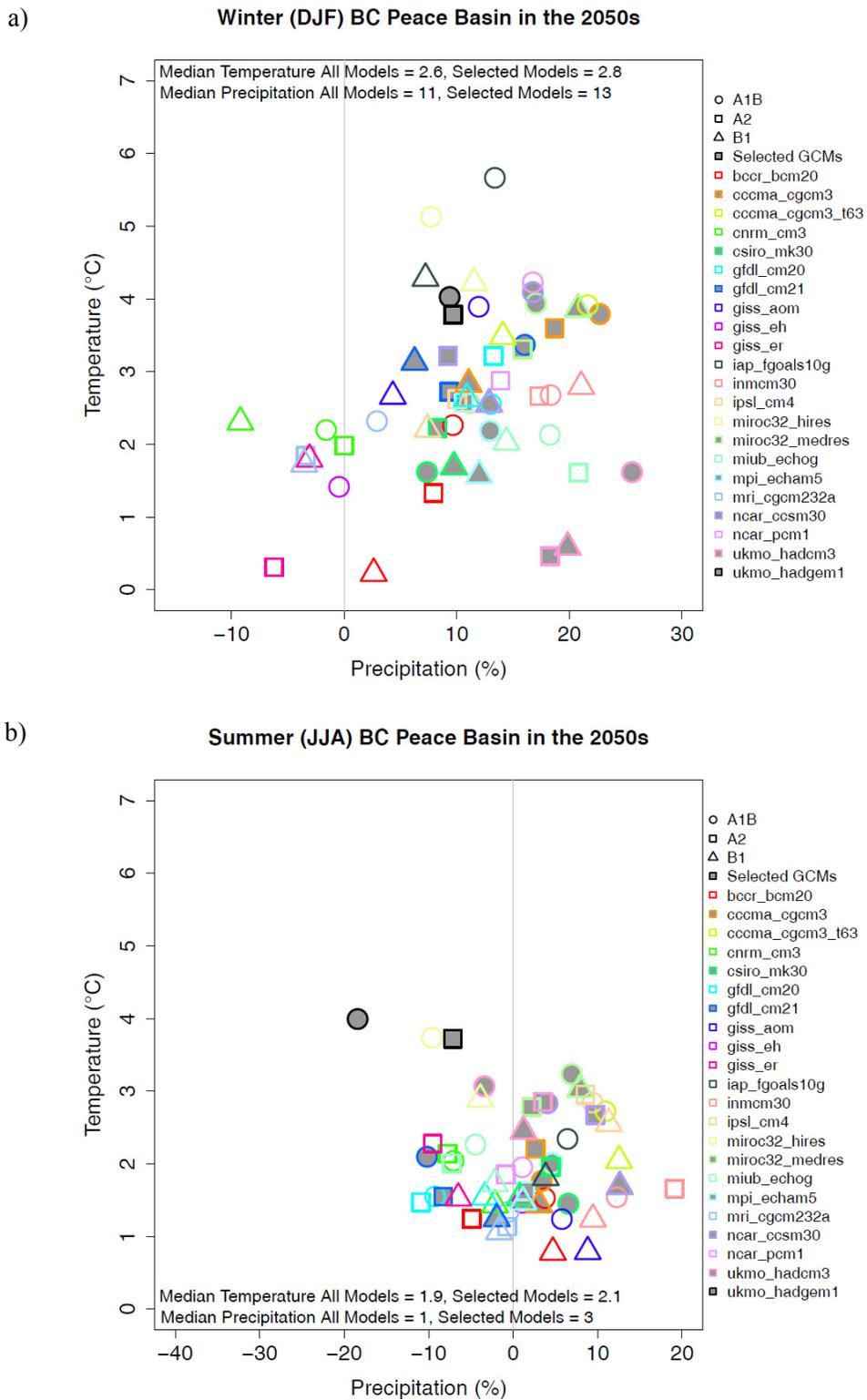
Figure 2-3. Projected temperature (°C) and precipitation (%) in the 2050s in winter (a) and summer (b) as a difference from 1961-1990 in the Peace Basin based on GCM output. Selected models are shown with grey infilling.

a)

Winter (DJF) BC Columbia Basin in the 2050s

b)

Summer (JJA) BC Columbia Basin in the 2050s
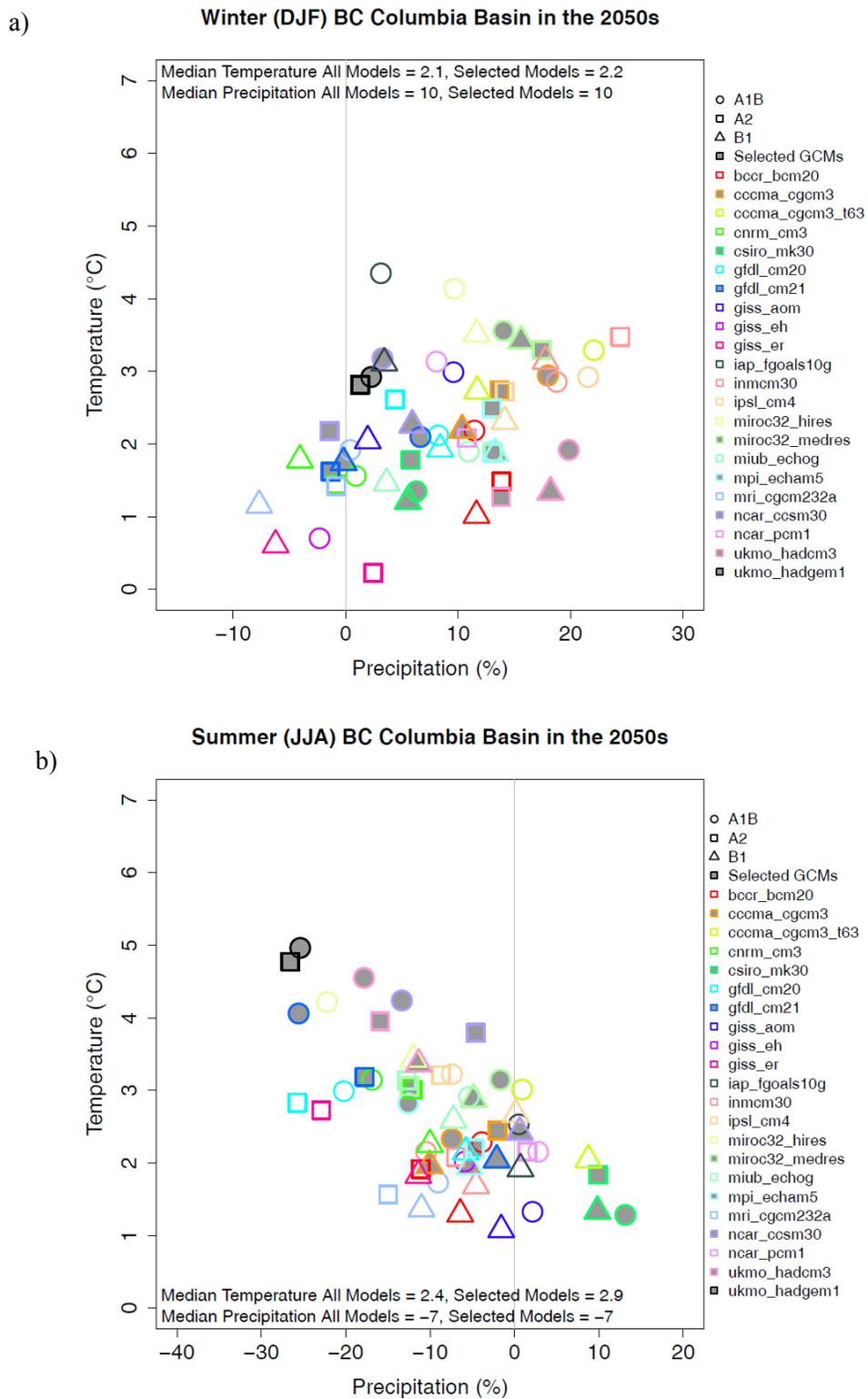
Figure 2-4. Projected temperature (°C) and precipitation (%) in the 2050s in winter (a) and summer (b) as a difference from 1961-1990 in the Columbia Basin based on GCM output. Selected models are shown with grey infilling.

2.3 Downscaling

Although many of the major components of the earth system are represented in GCMs, including ocean, atmosphere, and land surface, they are at scales such that fine topographic features such as mountain ranges or land-water interfaces that impact climate are not resolved. These features have an effect on the current climate and on how a region will be impacted by climate change. For example, although temperatures are projected to increase in a region, high elevation areas may also receive more precipitation and might remain cold enough to have precipitation continue to fall as snow versus rain. In a GCM, this type of elevation gradient would not be well represented. For example, a grid tile where there is a true elevation range of 200 m to 1200 m might be represented with an average elevation of 500 m in the model and the temperature would be represented with one average value over the entire tile area. Downscaling is a tool for relating information from coarse-scale GCMs (several ~100 km grids) to smaller scales (~10 km grids or specific locations) to more accurately represent regional variation in climate change.

Two main forms of downscaling exist: statistical and dynamical. Statistical downscaling draws upon empirical relationships between observed large-scale phenomena that are well simulated by models and observed variations in a target variable at the location of interest. Dynamical downscaling refers to a higher resolution climate model being embedded within a GCM, such as a regional climate model (RCM) or a limited-area model. The higher resolution model is forced at the boundary by the GCM and has parameterized physical atmospheric processes at this higher resolution. Some advantages of statistical downscaling over dynamic downscaling are that it is comparatively cheap and computationally efficient, based on standard and accepted statistical procedures. It is also able to directly incorporate observations (Wilby and Wigley 1997 and Fowler et al. 2007). Disadvantages of this approach are that it requires long and reliable observed historical data series for calibration, depends on the chosen predictors, does not include feedbacks in the climate system, assumes the established relationship between the predictor and predictand will hold in the future, and is affected by biases in the underlying GCM. Some non-linear forms of statistical downscaling, such as neural networks, include feedbacks between temperature and precipitation indirectly. The strength of the dynamical approach is that it produces responses based on physically consistent processes and produces finer resolution information from GCM-scale output that can resolve atmospheric processes on a smaller scale. However, it is computationally intensive, which limits the number of scenarios that can be downscaled and is strongly dependent on the GCM boundary forcing (Wilby and Wigley 1997 and Fowler et al. 2007).

This report focuses on statistical downscaling as it is applied to provide driving data at 1/16° spatial resolution for the VIC hydrologic model. As noted above, statistical downscaling is less computationally demanding than dynamical downscaling, which makes it advantageous for exploring the range of uncertainty due to multiple GCMs and emissions scenarios. Several approaches to statistical downscaling have been developed over the last couple of decades (Wilby and Wigley 1997; Xu 1999; Fowler et al. 2007). These techniques range from the simple delta-method to the more complex canonical correlation analysis (Fowler et al. 2007). Several inter-comparison studies of statistical downscaling techniques have been completed (Wilby and Wigley 1997; Xu 1999; Fowler et al. 2007; Maraun et al. 2010). Few techniques have been compared over the same spatial domain, using the same predictor variables and predictands, or against the same assessment criteria. This makes direct comparison of their relative performance difficult (Fowler et al. 2007). However, the bias-correction of climate model data was found to be an important aspect of using GCM or RCM data (Wilby et al. 2000; Hay and Clark 2003). The Bias Corrected Spatial Disaggregation (BCSD) statistical downscaling approach has been widely used and tested, especially in western North America (Wood 2002; Wood et al. 2004; Salathé 2005; Salathé et al. 2007; Maurer and Hidalgo 2008; Mote and Salathé 2009). It has been used extensively with the VIC hydrologic model. For these reasons, this technique has been used for this study and is described in detail below.

2.3.1 Bias Corrected Spatial Disaggregation (BCSD)

BCSD originated from the requirement to downscale ensemble climate model forecasts as input to a macro-scale hydrologic model to produce runoff and streamflow forecasts at spatial and temporal scales appropriate for water management (Wood et al. 2002). As the name implies, GCM data are bias corrected, downscaled to 1/8° or 1/16° horizontal resolution and then disaggregated to a daily time step for input to a hydrologic model, such as the Variable Infiltration Capacity (VIC) model (Liang et al. 1994). The BCSD method falls within a unique class of techniques where the predictor and predictand variables are the same (Rummukainen 1997), albeit of different scale. In this case, relationships between large-scale averages of temperature and precipitation and local-scale temperature and precipitation are used to develop empirical statistical relationships. BCSD is applied to monthly GCM data because daily data from GCMs was largely unavailable at the time this technique was developed (Wood et al. 2002). Additionally, daily GCM data would be much more cumbersome to process and challenging to bias correct due to mismatches between days of precipitation occurrence in GCMs versus actual occurrence (Wood et al. 2002), and the uncertainties in matching presence or absence of precipitation in the GCM to observed (Wehner 2010). The downscaling is performed in three steps: a) bias correction of the GCM fields using quantile mapping; b) "local scaling" of the corrected fields to the VIC grid, using calibration data from the overlapping period; and c) resampling of the daily historic record (at the VIC grid-scale) conditioned on the monthly averages of the locally scaled fields. Over the years, the BCSD method has been modified and adjusted to improve its ability to provide data for modelling projected changes to streamflow. The following will describe the approach as it has been applied in this study, taking time to note modifications that have been employed primarily by Dr. Eric Salathé (Jr.) of the University of Washington (Hamlet et al. 2010).

Before describing the technique step by step we will discuss the necessary input data. GCMs are bias corrected against gridded observations. These include gridded daily maximum and minimum temperature and precipitation at the spatial resolution of 1/16°, generated following Maurer et al. (2002) and Hamlet and Lettenmaier (1995). Daily station observations of minimum and maximum temperature and precipitation are collected from several agencies in Canada and the US, adjusted for the effects of topography with PRISM climatology for western Canada (Daly et al. 1994), interpolated using Climate Western North America (Climate WNA; Hamann and Wang 2005, Wang et al. 2006), and temporally homogenized to reduce any spurious trends or artifacts using long-term datasets. Daily wind speed surfaces are generated by re-gridding estimates of 10-m wind speed from the National Centers for Environmental Prediction-National Center for Atmospheric Research (NCEP/NCAR) reanalysis (Kalnay et al. 1996). See Schnorbus et al. (2011) for more details. This dataset will be referred to as the gridded-observed record. Average monthly minimum and maximum temperature and total monthly precipitation values of the gridded-observed record are produced in a pre-processing step of BCSD. As described above, due to the space needed to store large daily datasets, the inability of GCMs to represent daily patterns (presence or absence) of precipitation, and the uncertainties in matching percentiles in daily precipitation in GCMs to those in observed, or gridded-observed products, monthly GCM data forms the input for the BCSD technique. The strengths and limitations of the BCSD approach will be discussed below, but first we will outline the key steps in the technique. NCEP/NCAR reanalysis has a resolution ~1.9° comparable to that of GCMs; therefore it will be used as a surrogate GCM to demonstrate the steps in BCSD using 1950 to 1990 as the calibration period. Validation of this method over 1991 to 2000 will be described in the following section.

Steps in BCSD downscaling

Step – (1) – For each grid cell of a specific GCM and each calendar month we have a series of monthly mean temperatures for each year, *t*, of the base climate simulation, $T_{model}^{base}(t)$. Additionally, we have a time series of the gridded observed data (1/16°) aggregated to the resolution of the climate model (i.e., ~1.9° as for NCEP) in question for each month, $T_{obs}^{base}(t)$. For NCEP, the base case was 1950-1990 and 1991-2008 was considered as the future scenario. Before bias-correction is performed, trends are computed for the moving average of the monthly time series of the GCM (model) and the time series is de-trended (*Wood et al., 2004*). The observed and model time series are then used to construct a Cumulative Distribution Function (*CDF*) for the model, $C_{model}^{base}(T)$ and an inverse cumulative distribution function for the observed data, $\tau_{obs}^{base}(C)$. Example CDFs of temperature (Figure 2-5) are shown for NCEP and gridded-observed data aggregated to the model resolution for each month for one grid. The bias corrected GCM (model) temperature for a calendar month in year *t* for specific model grid cell is given by:

$$\hat{T}_{model}(t) = \tau_{obs}^{base}\{C_{model}^{base}[T_{model}(t)]\}$$

where the CDF, $C_{model}^{base}(T)$, denotes the fraction of years in the time series where temperature is less than *T* for the calendar month under consideration and the $T_{model}(t)$ is the series of simulated monthly mean temperatures for the full simulation (Salathé et al. 2007). All models downscaled using BCSD for the VIC hydrologic model study were calibrated over 1950-2000 (base). After bias-correction, trends computed on the monthly time series are replaced. This process is repeated for each model grid cell in the domain and each calendar month and is the same for precipitation (Figure 2-6). Time series of the original model data (NCEP in this case), the gridded-observed data aggregated to the model resolution (~1.9°) and the bias-corrected model data are shown for each month for temperature (Figure 2-7) and precipitation (Figure 2-8) for a selected grid location.

The above describes the approach for the majority of the cases. As there are more GCM data available than observations, there are some occurrences where the GCM values fall above or below the range of observed values. In that case, the observed CDF is approximated by a Weibull function and the values are extrapolated accordingly. For low precipitation, an Extreme Value Type III (Weibull) function is used, with a minimum lower bound of zero, whereas for extreme high precipitation an Extreme Value Type I (Gumbel) distribution is employed. For temperature, a normal distribution is used for both minimum and maximum.
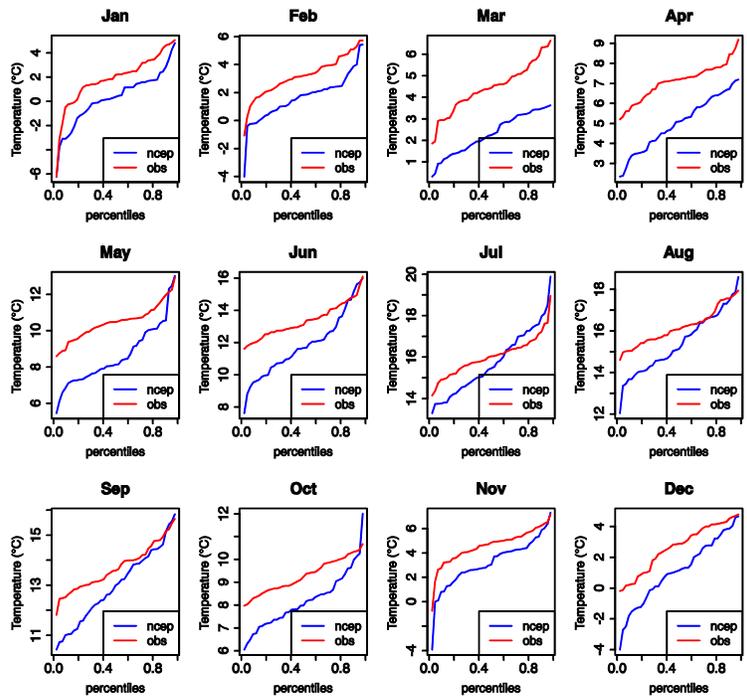
Figure 2-5. Cumulative distribution functions of monthly temperature (°C) from the NCEP model (blue line) and aggregated gridded-observations (red line) at a selected grid cell.
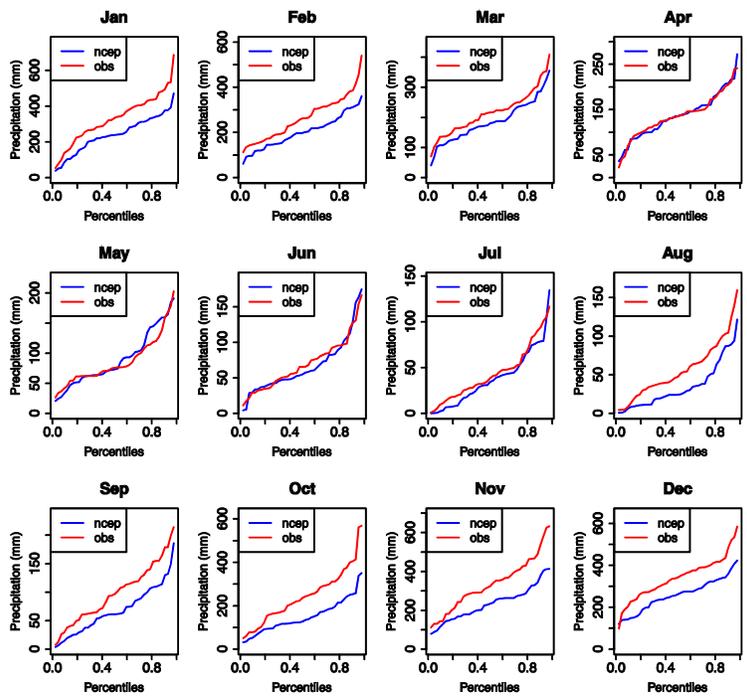
Figure 2-6. Cumulative distribution functions of monthly precipitation (mm) from the NCEP model (blue line) and aggregated gridded-observations (red line) at a selected grid cell.

19
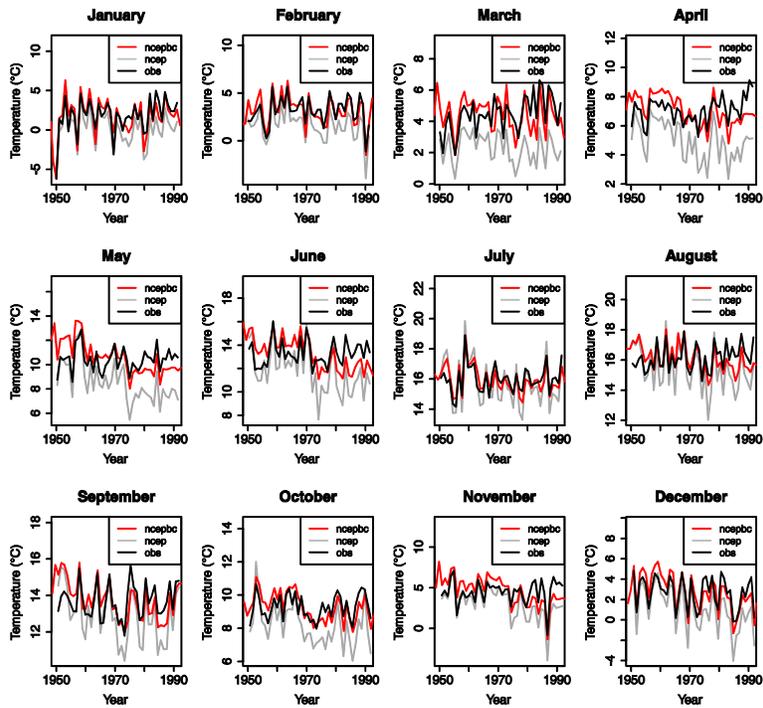
Figure 2-7. Time series of monthly temperature (°C) from the NCEP model (grey line), aggregated gridded observations (black line), and bias-corrected NCEP model (red line) at a selected grid cell.
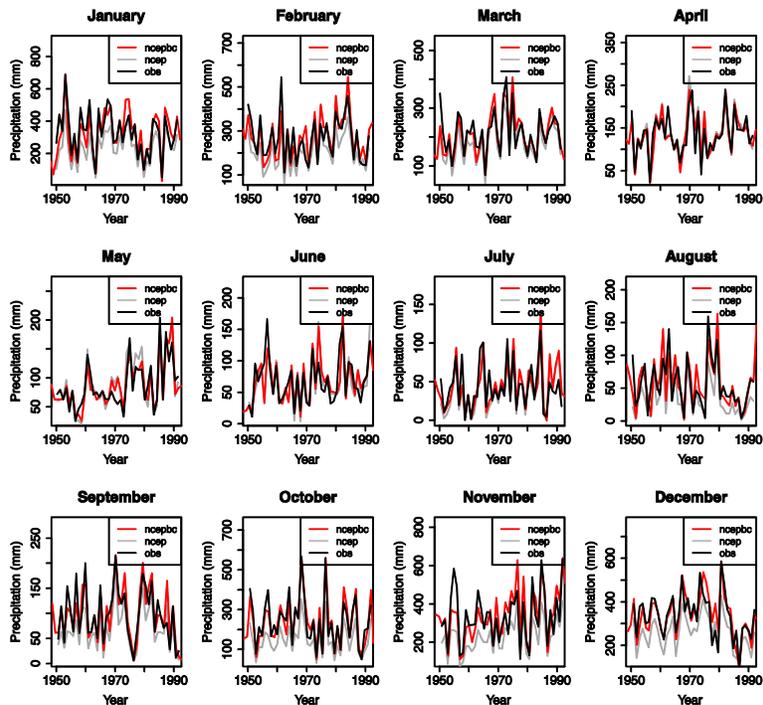
Figure 2-8. Time series of monthly precipitation (mm) from the NCEP model (grey line), aggregated gridded observations (black line), and bias-corrected NCEP model (red line) at a selected grid cell.
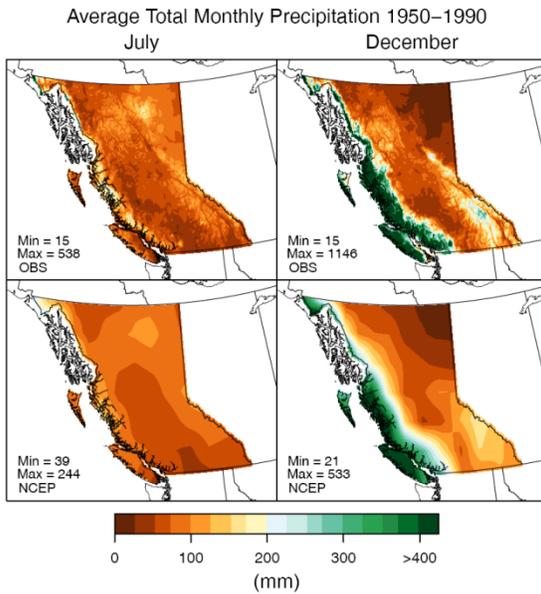
Figure 2-9. Average monthly precipitation (mm) over 1950-1999 for the gridded-observations (top) and from the interpolated NCEP model (bottom) for July (left) and December (right).
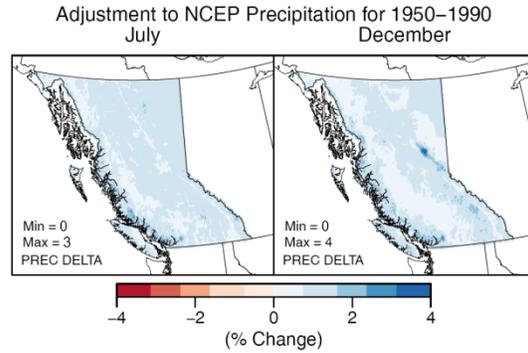
Figure 2-10. Percentage precipitation adjustments required to locally scale monthly bias-corrected NCEP data to average monthly precipitation (mm) from gridded-observed data for same period for July (left) and December (right).

Step – (2) – the bias corrected monthly temperature and precipitation from the model simulations are spatially downscaled by interpolating monthly anomalies established over the historical record (1950-1999) to the target higher resolution of the application (1/16°). This step is referred to as 'local' scaling because the large-scale simulated precipitation at each local grid point is simply multiplied by a monthly scale factor, or added/subtracted for temperature. 'Local' scaling is designed to remove the long-term bias between the large-scale simulated precipitation or temperature and the observed value at that grid point. Fitting is performed independently for each month. Average monthly precipitation for July and December for the gridded-observed data and the interpolated model (NCEP) are shown in Figure 2-9. The large-scale simulated precipitation at each local gridpoint is multiplied by an adjustment factor derived during the fitting period, shown in Figure 2-10 for both months for the NCEP case.

This process can be described in mathematical terms as follows. If $P_{mod}(x,t)$ is the simulated large-scale monthly mean precipitation containing a location *x* and at time *t* in months '*mon*', then the downscaled monthly mean precipitation $P_{ds}(x,t)$ is:

$$P_{ds}(x,t) = P_{mod}(x,t)\frac{\langle P_{obs}\rangle_{mon}}{\langle P_{mod}\rangle_{mon}}$$

where $\langle...\rangle_{mon}$ is the monthly mean taken over the fitting period or calibration period where the gridded-observed dataset and the historic run of the GCM over lap at the 1/16° grid scale (Salathé 2005). The fitting is performed independently for each month. Similarly air temperature is scaled by adjusting the bias corrected GCM or NCEP data, but with an additive adjustment instead. Average monthly minimum temperature for the gridded-observed data and interpolated average monthly average temperature for the model (NCEP) are shown in Figure 2-11.
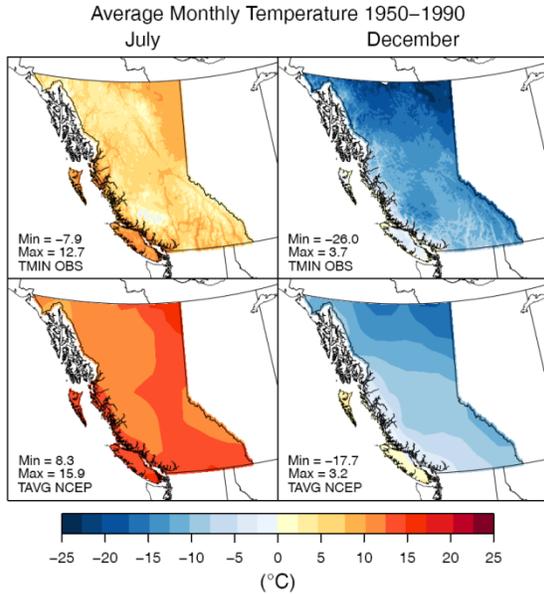
Figure 2-11. Average minimum monthly temperature (°C) over 1950-1999 for the gridded-observations (top) and average monthly temperature from the interpolated NCEP model (bottom) for July (left) and December (right).
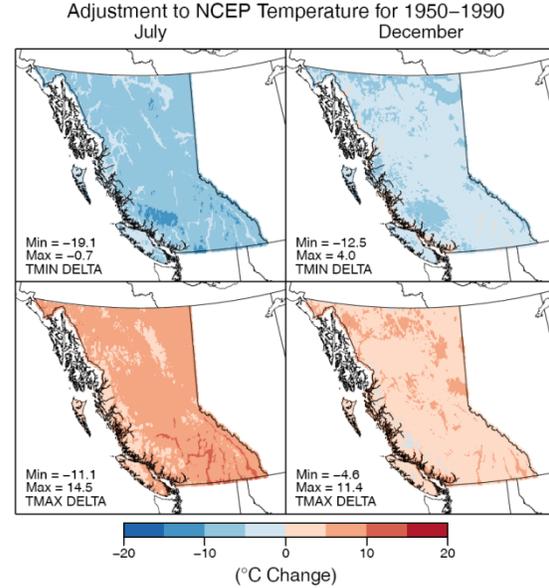
Figure 2-12. Absolute temperature adjustments required to match bias-corrected NCEP data to average minimum and maximum temperatures (°C) from gridded-observed data for same period for July and December.

The minimum and maximum scaling for the model is done by comparing average temperature in the model to minimum and maximum temperatures from the gridded-observed data because only average temperature is available for most models. The locally scaled monthly mean surface temperature is given by

$$Tmin_{ls}(x,t) = T_{mod}(x,t) + [\langle Tmin_{obs}\rangle_{mon} - \langle T_{mod}\rangle_{mon}]$$

$$Tmax_{ls}(x,t) = T_{mod}(x,t) + [\langle Tmax_{obs}\rangle_{mon} - \langle T_{mod}\rangle_{mon}]$$

where $\langle...\rangle_{mon}$ is the monthly mean taken over the fitting period or calibration period where the gridded-observed dataset and the historic run of the model overlap at the 1/16° grid scale (Salathé 2005). The local-scale temperature is generated by removing the monthly bias in the large-scale mean. $Tmin_{ls}(x,t)$ and $Tmax_{ls}(x,t)$ values required to correct NCEP based on comparison to gridded-observations over the 1950 to 1990 period are shown for each VIC grid cell in BC (1/16°) in Figure 2-12. Since the local temperature is found from the large-scale temperature simply by adding or subtracting a monthly bias in the mean, it can be thought of as a lapse-rate correction. Differences in temperature are most likely due to the elevation difference of the local grid point (1/16°) relative to the GCM grid. If the lapse rate is strongly affected by climate change this assumption will break down (Salathé 2005).

Step – (3) – The daily time series is created by temporally downscaling the bias corrected, locally scaled, monthly time series (1950-2100) by scaling (for P_{tot}) or shifting (for T_{min} and T_{max}) month-long daily patterns resampled from the 1/16° historic record (1950-2006; Wood et al. 2002). This temporal selection applies a stochastic technique, wherein a historic month in the observed-gridded record is chosen randomly except for a check to ensure a relatively wet historic month is picked when a wet month is being downscaled. The temperatures are then chosen from the same month to match the one selected for precipitation and both are selected for the entire region of interest, such as BC, at 1/16° for that month to preserve a degree of synchronization in the weather components driving the hydrologic response (Wood

et al. 2004). The daily variability from the selected month is imposed on all gridpoints while preserving the downscaled monthly mean from the model (NCEP in this case). This disaggregation yields daily minimum (T_{min}) and maximum (T_{max}) temperatures. The observed sequence of T_{min} and T_{max} for the selected month are shifted by a constant factor τ such that the shifted daily mean temperature

$$T_{mean} = (T_{min} + T_{max}) \times 0.5 + \tau$$

averaged over the month, equals the downscaled monthly mean surface temperature from the model (NCEP in this case). Thus, the diurnal range is taken from the analogue month and is not subject to climate change (Salathe et al. 2005). This is a necessary assumption as daily GCM data is not applied in this process, in spite of evidence that the diurnal temperature range has changed in the past and is predicted to change in the future. Minimum temperature has increased faster than maximum temperature in many areas in BC (Rodenhuis et al. 2009).

Lastly, the resulting downscaled daily time series is checked and corrected against a prescribed threshold, defined as 150% of the observed maximum precipitation for each cell in the gridded-observed record in that month, to ensure no anomalous large daily precipitation events take place and to spread out very large daily precipitation values into one or more adjacent days (Hamlet et al. 2010). This is a potential downfall of this method as future daily precipitation values are not permitted to be greater than those in the past. Daily wind speeds are taken without adjustment from the gridded observed values for the selected year and month for the BCSD downscaled product (Wood et al. 2002). In other words, no wind information from the GCM/model is used in BCSD.

Daily precipitation (Figure 2-13) and minimum and maximum temperature (Figure 2-14a and Figure 2-14b) are shown for a select 1/16° grid cell as downscaled from NCEP using BCSD for 1991-2000. Since daily data was not used to calibrate the technique this is an independent validation of the daily data produced by this technique. This period of record was not included in the calibration of BCSD to NCEP and therefore, can be considered a unique validation period. The timing and magnitude of daily precipitation and daily minimum and maximum temperatures are within the range of gridded-observations (Figure 2-13, Figure 2-14a and Figure 2-14b). This location is given as an example and is not necessarily representative of the match between gridded-observations and BCSD downscaled NCEP at other locations in the province.

Given the decision to not downscale daily information from the GCM with this technique, it is important to note that the daily characteristics are an artifact of the temporal re-sampling procedure and do not directly reflect changes to statistical properties of daily weather projected by individual GCMs. For example, because the frequency of precipitation is re-sampled from the historic record, the frequency of wet/dry days and duration of wet spells does not change. However, application of daily GCM data is more limited in published studies than monthly and because of this there are those in the user community who are less likely to trust daily GCM data. Additionally, strategies for statistically downscaling daily GCM data would include more uncertainties than working with monthly data. Nevertheless, daily or sub-monthly GCM data would have to be downscaled to study changes in hydrologically pertinent variables such as the duration of wet and dry spells.
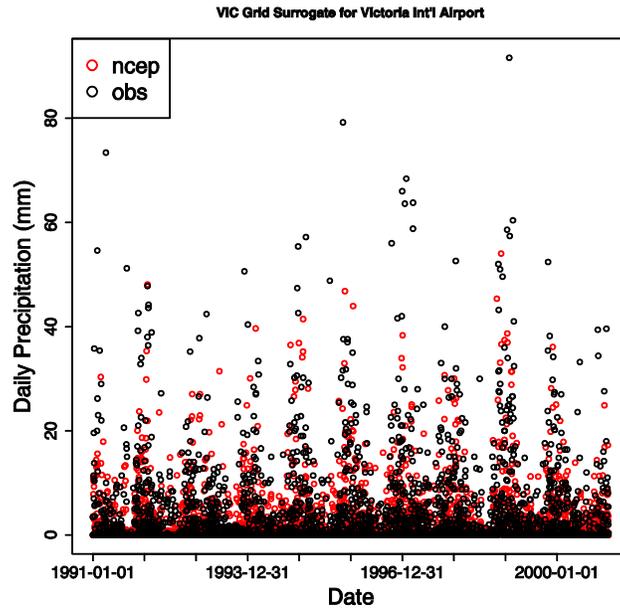
Figure 2-13. Daily precipitation (mm) downscaled using BCSD from the NCEP model (red circles) and gridded-observations (black circles) at a selected 1/16° grid cell from January 1, 1991 to December 31, 2000.
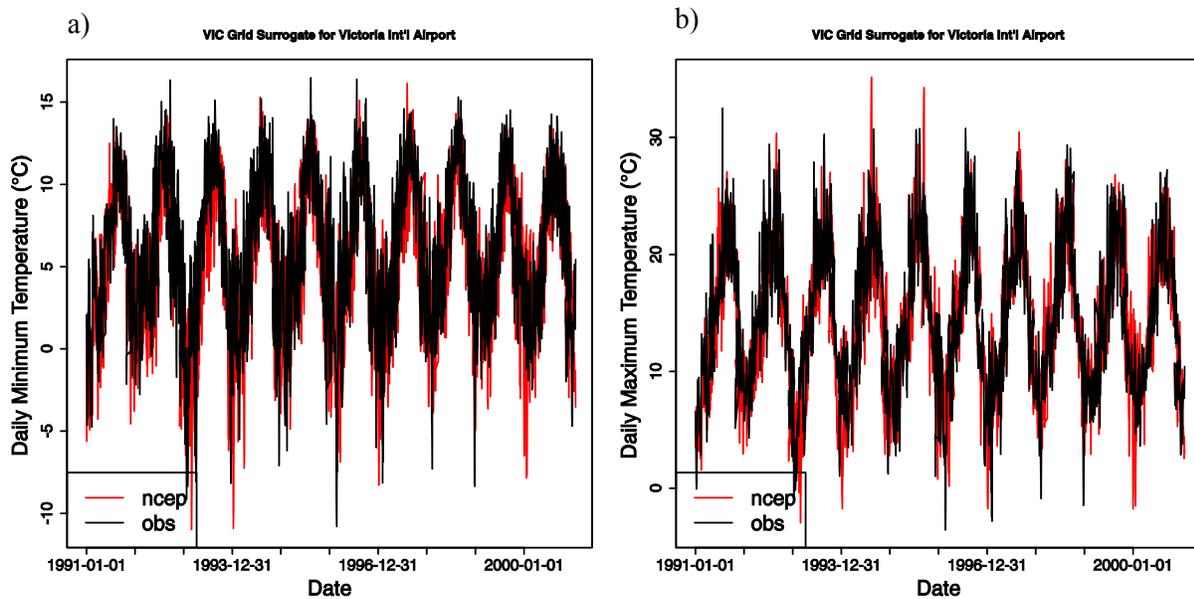
Figure 2-14. Daily minimum (a) and maximum (b) temperature (°C) downscaled using BCSD from the NCEP model (red lines) and gridded-observations (black lines) a selected 1/16° grid cell from January 1, 1991 to December 31, 2000.

Strengths of this method include its ability to explicitly capture the transient nature of the emissions scenarios, which is useful for capturing the trend in the regional climate and hydrologic response. Projected changes in the monthly signal are useful for many planning purposes. This method has also been shown to perform well when results tuned to the cold phase of the Pacific Decadal Oscillation (PDO) are applied on the warm-PDO and vice versa, suggesting it functions in altered climates and may work in future climates (Salathé et al. 2007), although the difference between the cold and warm PDO are not of the same magnitude as the forced signal at the end of the 21st century. The trends in the climate projection and the modes/shifts in climate variability are preserved in the transient downscaling of monthly GCM time-series (Mote and Salathé 2009). A limitation of the method is if GCMs are of poor quality, the process carries this information forward, although the case would be the same with many downscaling approaches. Thus, the approach requires careful screening of the GCMs. As we have done in this study, screening models to ensure that they closely reproduce important statistics such as sequencing and variability over the area of interest and over the historical record, is important especially at small spatial scales (Hamlet et al. 2010).

Alternative approaches to projecting future changes in streamflow using BCSD include other statistical downscaling methods, such as Expanded Downscaling (Bürger, 1996; Bürger et al. 2009) or Tree-GEN (Stahl et al. 2008). These are commonly used to downscale to a station and therefore their outputs would have to be interpolated in some way to drive a distributed hydrologic model like VIC. Dynamical downscaling, also referred to as regional climate modelling, could also be used to project future changes in streamflow, or a combination of the two. A Regional Climate Model (RCM) represents the local responses to climate change with higher resolution than a GCM, which may be critical to applications in regions of complex terrain and land-water contrasts (Mote and Salathé 2009). Via an RCM, GCM output can be dynamically downscaled and can be explored directly at the native resolution of the RCM within a fully coupled land-ocean-atmosphere environment. Such an approach has also been pursued at PCIC as a parallel project. Discussion of those results is beyond the scope of this report and the reader is referred to Rodenhuis et al. (2010) for further details. Much like GCMs, RCMs are biased and need to be statistically downscaled before using RCM results to drive a hydrologic model. Work in this field is still evolving and not yet common practice, but has great potential (Leung et al. 2003; Wood et al. 2004).

(BLANK)

3. Validation

The BCSD method has been tested at 1/8° resolution over several regions in North America, most of which were in the US. It has been compared to other statistical methods such as linear interpolation (LI), spatial disaggregation (SD) and constructed analogues (CA) as well as dynamic downscaling approaches (Wood et al. 2004; Salathé et al. 2007; Maurer and Hidalgo 2008). One approach to testing the BCSD output is to run it through the VIC hydrologic model and compare simulated streamflow to observed streamflow. In one case, BCSD successfully reproduced the main features of the observed hydrometeorology from both a GCM and an RCM due to the bias correction step that made it superior over the LI and SD approaches (Wood et al. 2004). In another study, the CA and BCSD approaches were compared for their ability to produce continuous, gridded time series of precipitation and surface air temperature over the western US. CA downscales daily large-scale data directly and BCSD downscales monthly data, and generates daily values with a random resampling technique (Maurer and Hidalgo 2008). Both have comparable skill in producing downscaled, gridded fields of precipitation and temperature at a monthly time step. The CA method was better than BCSD in reproducing low temperature extremes in fall and winter and high temperature extremes in summer. The ability to produce skillful downscaled daily data was found to rest with the skill of the GCM to produce daily data (Maurer and Hidalgo 2008).

The above mentioned studies have tested BCSD at 1/8° resolution over the US. In this study we validated the BCSD results at the 1/16° resolution over BC by comparing our downscaled gridded temperature and precipitation to our gridded-observed dataset. NCEP/NCAR reanalysis data was used as the surrogate GCM. NCEP serves as an appropriate surrogate GCM due to its comparable resolution of approximately 1.9° per side and its reanalysis of observations. Additionally, as a reanalysis product, the timing of annual variability in NCEP should match those in the observations, which makes it meaningful to compare results of downscaling NCEP to gridded observations from year to year. By downscaling NCEP with BCSD we can test the strength of the BCSD method without having to overcome the strong biases found in many GCMs. The technique will be calibrated over 1950 to 1990 and validated over 1991 to 2000. This is a relatively short validation period for a region where there is such large inter-annual variability in precipitation, but was all that was available with the current datasets. These experiments tested the skill of the BCSD technique at a higher resolution in a hydro-climatically complex region, where some of the largest climate changes are projected due to the snow-albedo effect (Christensen et al. 2007).

3.1 Spatial Analysis of Monthly Average Conditions

First, average raw NCEP data (~1.9°) was compared to gridded-observations (~1/16°) for July and December over the 1950 to 1990 period. Temperature patterns and magnitudes were similar between the two datasets for July and December, but NCEP lacked detail in comparison to higher resolution gridded-observations (Figure 3-1). In July, both datasets displayed warm average conditions in the southern and northeastern portions of the province (12.5°C to 15°C) and moderate temperatures in the northwest and central coast (2.5°C to 12.5°C), although colder conditions (2.5°C to 5°C) were more pervasive according to NCEP in the northwest (Figure 3-1a). The largest differences between the two datasets were found in regions with large elevation gradients, where high elevations remained below 5°C and some of the valleys reached temperatures greater than 20°C on average in July (Figure 3-1a). In December, both datasets present cold average conditions (-25°C to -10°C) in the north part of the province, below freezing conditions (-10°C to 0°C) in the central part of the province, and near zero conditions (-5°C to 5°C) along the central coast and south coast (Figure 3-1a). Again, primary differences resulted from lack of resolution in NCEP that prevented adequate representation of strong elevation gradients; valleys were primarily ~5°C warmer according to the gridded observations than the corresponding NCEP tile and mountain peaks were ~3°C cooler. Elevations of BC as represented in the gridded-observations and

NCEP are shown in Figure 3-2. The range in elevation for NCEP is less than half that of the elevation in the gridded-observations. However, some noticeably warmer areas (~2°C warmer) were found in NCEP on the west coast islands, suggesting the reanalysis product is warmer than the gridded-observed data, possibly due to different stations being included in the gridded-observation dataset than used in NCEP. There could be a lower number of observations in the gridded-observed product in these regions.
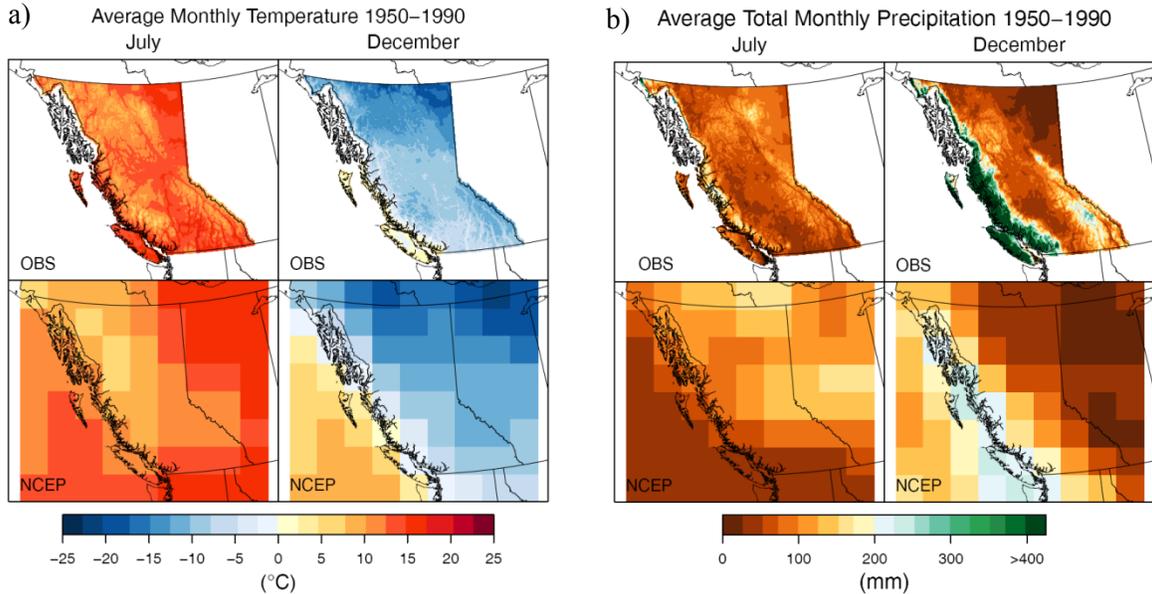
Figure 3-1. Average temperature (a) and precipitation (b) in July and December over 1950-1990 for NCEP (bottom row) in its native 1.9° resolution as compared to the gridded-observed (1/16°) climatology for the same period (top row).
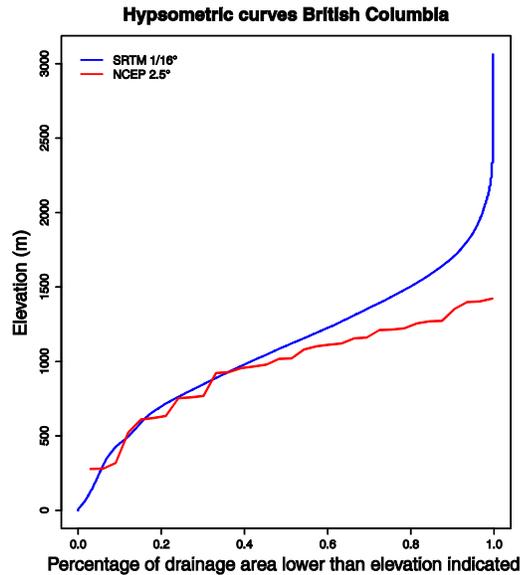
Figure 3-2. Elevation of BC as represented by 1/16° Shuttle Radar Topography Model (SRTM) Digital Elevation Model (DEM) applied to create gridded-observations and 2° DEM applied in NCEP reanalysis.

Precipitation varied in its spatial pattern and magnitude between the two datasets for July and December. In July, the range in the magnitude of precipitation was similar in both datasets (~0 to 200 mm). However, much of the variation in precipitation was not represented from north to south, east to west and from low to high elevation in NCEP as it was in the gridded-observations (Figure 3-1b). In December, precipitation is underestimated by NCEP along the coastline and in the interior mountains (Figure 3-1b). Maximums of 275 mm in the coastal regions found in NCEP do not compare with maximums of 1220 mm outlined in the observed, although regional averages at the NCEP grid box scale might be correct. Additionally, some of the drier regions in the province, such as the lee-side of the Coast Mountains and northeast are not represented by NCEP because precipitation values are greater than those from gridded-observations by more than 100 mm in some places.

To test the BCSD procedure in BC, validation was carried out over 1991 to 2000, which is distinct from the 1950 to 1990 calibration period. Over 1991 to 2000, July temperature differences ranged from -2.2°C to 0.6°C and had a median difference of -0.3°C. Cold biases prevailed in the northwest and south central area of the province with differences of up to -2.2°C and warm biases remained in the northeast corner of the province with differences of up to 0.6°C in this month. December temperatures were within -1.8°C to 0.4°C and had a median difference of -0.6°C (Figure 3-3a). Biases were primarily negative and close to zero, except for some areas of the coast where warm biases (~0.4°C) were found. For precipitation, BCSD downscaled NCEP results were within -35% to 69% of gridded-observations for the majority of the province in July (Figure 3-3b). Dry areas were found in the middle section of the province and on the south coast of Vancouver Island and wet areas were found in the northeast and south. NCEP results were dry in July on average over BC in comparison to gridded-observations based on the median by -4%. In December, differences were between -49% and 59% and were unbiased on average over the province according to the median (0%). Wet areas remained along the western portion of the province and dry areas along the east, with maximum dry bias of -49% situated in the northern tip of the Columbia basin near the BC-Alberta border (Figure 3-3b).

Based on the median, downscaled results were representative of observed average temperature and total precipitation for July and December when BCSD downscaled NCEP results were compared to gridded-observed data over the 1991 to 2000 period. In some areas where the NCEP BCSD results were drier than gridded-observations, gridded-observations were found to have a trend over 1950-2000 that was not captured by calibrating BCSD to 1950-1990. The trend in the gridded-observations might have reflected increases in precipitation caused by a shift in the PDO combined with climate warming, or might be a result of changes to the station mix caused by adding new stations later in the record. This will have to be looked into further to rule out issues with the gridded-observations.
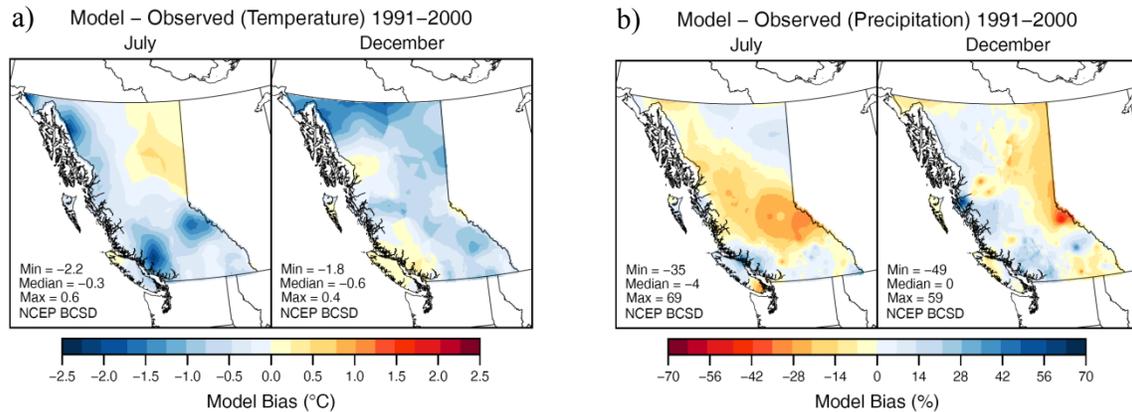
Figure 3-3. The difference between BCSD downscaled NCEP and gridded-observed values for (a) temperature as NCEP BCSD minus OBS (°C) and (b) precipitation as NCEP BCSD minus OBS divided by OBS (%) are shown for July and December.

3.2 Comparison of Daily Results via Indices

Daily downscaled values result from re-sampling daily values from the gridded-observed record. Selected months in the gridded-observed record are adjusted to match monthly values of the bias-corrected, locally-scaled GCM (or NCEP) data. Thus, the frequency of days with or without precipitation will match those in the months sampled from the gridded-observed record and is not related to the model. Given the stochastic nature of this process, one is left to wonder how realistic resulting daily values are. One way to evaluate the skill in representing daily values is to compare the BCSD downscaled NCEP values to those from the VIC gridded-observed dataset via climate indices at the same location. The climate indices investigated in this case are part of *Climdex*. Climdex is a common climate indices package that computes values for 29 core indices based on daily precipitation, minimum and maximum temperature (Peterson 2005). These indices describe the daily extremes, such as the number of heavy precipitation days denoted as days where precipitation is greater than 10 mm or percentage of days when maximum temperature is greater than the 90th percentile. To evaluate extremes, long time periods are required (i.e., > 10 years). Thus, the following analysis pertains to the 1961 to 2006 period of record, which includes part of the calibration period (1950 to 1990). In the previous section, validation of BCSD results was carried out for a separate validation period, but in this case it was necessary for the validation period to overlap with the calibration period to provide adequate records to explore extremes. BCSD results were evaluated for the following 12 indices, a subset of the 29 core indices available (Table 3-1):

Table 3-1. Definition of Climdex climate indices applied in this study.

ID	Indicators Name	Definitions	UNITS
R10	Number of heavy precipitation days	Annual count of days when PRCP>=10mm	days
R20	Number of very heavy prec. days	Annual count of days when PRCP>=20mm	days
R95p	Very wet days	Annual total PRCP when RR>95th percentile	mm
PRCPTOT	Annual total wet-day precipitation	Annual total PRCP in wet days (RR>=1mm)	mm
TN10p	Cool nights	Percentage of days when TN<10th percentile	days
TN50p	(not an extreme index)	Percentage of days when TN>50th percentile	days
TN90p	Warm nights	Percentage of days when TN>90th percentile	days
TNn	Min Tmin	Monthly minimum value of daily minimum temp	°C
TX10p	Cool days	Percentage of days when TX<10th percentile	days
TX50p	(not an extreme index)	Percentage of days when TX>50th percentile	days
TX90p	Warm days	Percentage of days when TX>90th percentile	days
TXx	Max Tmax	Monthly maximum value of daily maximum temp	°C

BCSD daily values for one grid are compared to VIC gridded-observations at the same location and the nearest climate station (Victoria International Airport – 1018620). For the temperature variables *TN10p*, *TN50p*, *TX10p*, and *TX50p* the BCSD downscaled NCEP results match the explained variance (EV) of the VIC gridded-observations and that of the station data at the 99% confidence level (Table 3-2). An EV of 80% means that 80% of all observed variation is simulated by the BCSD downscaled NCEP. Percentiles are calculated over the 1961-2006 period. Review of the plots for these variables shows that, although the years when the percentage days less than the 10th percentile or greater than the 50th percentile do not coincide between the BCSD results and the observations (gridded and station data), the variability and range between all three datasets is similar (Figure 3-4 and Figure 3-5). Due to the stochastic nature of the temporal disaggregation process that produces daily values we would not expect the timing of events in the BCSD results to match those in observations. The explained variance for the BCSD for *TN90p*, *TX90p*, *TNn* and *TXx* match the gridded-observed data at the 99% confidence interval, but not when compared to the station observations. This suggests that gridded-observations do not represent the temperature extremes found in the station data and since BCSD is calibrated against the gridded-observations it too does not have the same variability as the station data. The monthly minimum (maximum) value *TNn* (*TXx*) of daily minimum (maximum) temperature is not comparable to the station data at the 99% confidence interval (Table 3-2). A few events where temperatures are low in the observed records for *TNn* are not reproduced by downscaled NCEP data (Figure 3-4). *TXx* temperatures from downscaled NCEP are less than both observational datasets for most of the record by 5°C or 6°C in some places (Figure 3-5). Because the monthly maximum value of daily maximum temperature is being downscaled from mean monthly GCM values it is hard to reproduce with the BCSD process.
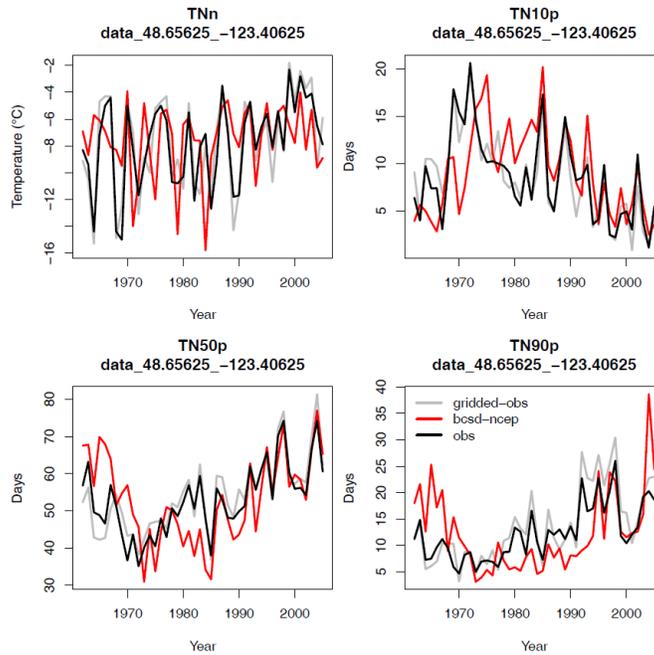
Figure 3-4. BCSD downscaled NCEP (red) compared to VIC gridded-observations (grey) and Victoria International Airport climate station (black) for four minimum temperature indices (TNn (°C), TN10p (days), TN50p (days), TN90p (days)).
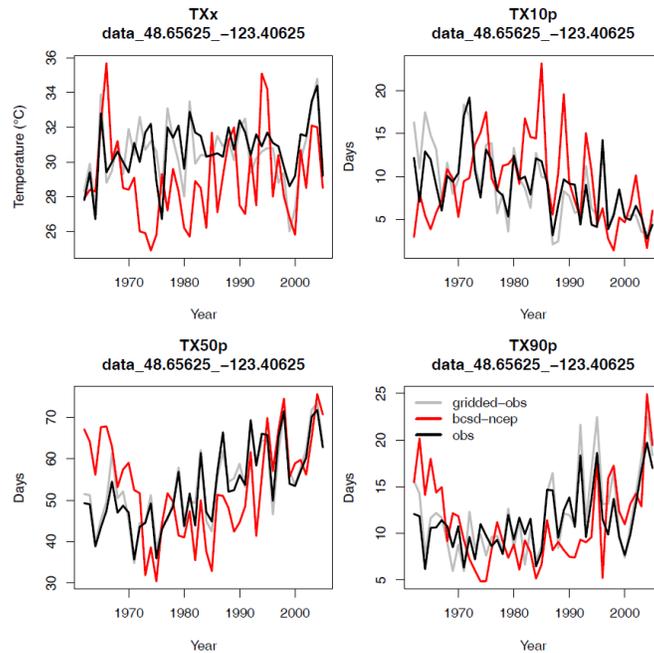
Figure 3-5. BCSD downscaled NCEP (red) compared to VIC gridded-observations (grey) and Victoria International Airport climate station (black) for four maximum temperature indices (TXx (°C), TX10p (days), TX50p (days), TX90p (days)).

Table 3-2. Explained variance (EV) for each variable in Table 3-1 when BCSD downscaled NCEP is compared to gridded-observations (EV1) and to station observation (EV2). When values are shown it indicates downscaled NCEP values are within 99% confidence interval of gridded-observations. Percentiles are calculated over 1961-2006 for EV1 and over 1991-2006 for EV2. The total variance is given by 100 – EV.

ID	R10mm	R20mm	R95p	PRCPTOT	TN10p	TN50p	TN90p	TNn	TX10p	TX50p	TX90p	TXx
Units	days	days	mm	mm	days	days	days	°C	days	days	days	°C
EV1	22	-15	-51	29	-79	-228	-227	-45	-118	-158	-126	-440
EV2	32		-87	36	-40	-124			-131	-178		

Various annual statistics for daily precipitation from BCSD downscaled NCEP are similar to the gridded-observed and station data (Figure 3-6). This could be because daily values are created through selection of months from the gridded-observed record based on whether their precipitation totals are relatively wet or dry to better match the month which is being downscaled from the model (NCEP in this case). Temperature values are derived from the same months picked for precipitation. Downscaled NCEP values have similar variance to the gridded-observed and station data for all four variables (R10mm, R20mm, R95p and PRCPTOT), except downscaled R20mm does not have the same variance as the station data. The R20mm events are not replicated by the BCSD NCEP results or the gridded-observations. Therefore, it can be assumed that the events recorded by the station were not captured by the process used to create the gridded-observed values and the BCSD process was therefore not able to replicate these events.
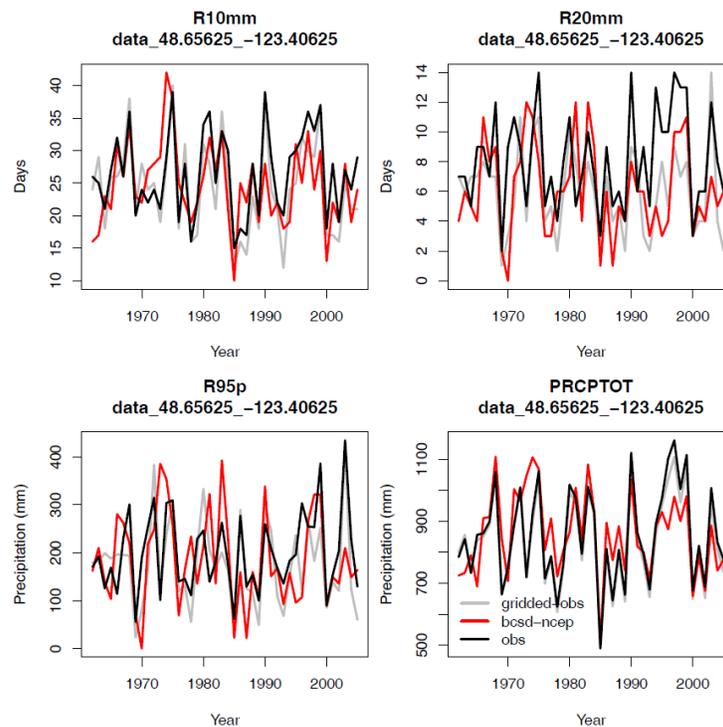
Figure 3-6. BCSD downscaled NCEP (red) compared to VIC gridded-observations (grey) and Victoria International Airport climate station (black) for four precipitation indices (R10mm (days), R20mm (days), R95p (mm), PRCPTOT (mm)).

This analysis is based on NCEP data, which should have similar values to observed records because it is a reanalysis product, although it is originally produced at the 1.9° scale and at such a scale is not able to capture the local-scale events. Additionally, it should be noted that because the daily information does not come from the GCM, but instead from the gridded-observed data, the frequency of precipitation events modelled in GCMs will not be captured and transitions to more frequent or less frequent precipitation in the future under climate change will be lost.

Based on these results, it seems that BCSD is able to reproduce the statistics of the gridded-observed record to which it is calibrated. BCSD daily results also have variance close to that of station data for some of the variables investigated, in spite of the somewhat stochastic process used to derive daily values. This suggests that BCSD downscaling produces physically realistic historical daily results.

This is only one limited test of daily values produced by the BCSD method. It should be taken into consideration that area-averaged values always reduce the magnitude of extremes (Haylock et al. 2008). Therefore, comparing station data to spatially averaged gridded downscaled results is a hard test. Since the daily values are derived by resampling the historical gridded observations and adjusting them based on the bias-corrected, locally-scaled monthly GCM projections, this approach does not explicitly capture changes to future daily extremes that are projected by the various GCMs. In studies that require daily data to analyze future droughts or flood events, other downscaling methods should be sought.

4. Results and Discussion

This section will discuss BCSD results as an ensemble and by emissions scenario to explore the range in possible futures and their response over BC. Additionally, to better understand the result of applying BCSD to a GCM, CGCM3 A2 projections downscaled using BCSD are compared to raw GCM projections for average annual temperature and annual total precipitation in BC. This model was selected because it was used in *Climate Overview*: *Hydro-climatology and Future Climate Impacts in British Columbia* (Rodenhuis et al. 2009), the first report of the Hydrologic Modelling Project.

4.1 Spatial - Multiple Scenarios

High-resolution (1/16°) BCSD downscaled results are presented for annual and seasonal average temperature and total precipitation anomalies in the 2050s (2041-2070) as a difference from 1961-1990 over BC. Minimum, maximum, average and median values are computed for the 23 projection ensemble which is composed of eight models (CCSM3, CGCM3.1(T47), CSIRO-Mk3.0, ECHAM/MPI-OM, GFDL2.1-CM2.1, UKMO-HadCM3, UKMO-HadGEM1 and MIROC3.2 (medres)) all run under three emissions scenarios (B1, A1B and A2) except for UKMO-HadGEM1, which was not run under B1. In the following section, we will describe the range in projected changes across BC and its regions, both annually and seasonally for this ensemble.

By the middle of the 21st century (2050s) annual temperatures are estimated to increase by 2.3 °C for the median of the ensemble on average over BC. Projected increases in annual temperature range from 1.4 °C to 3.7 °C over the province based on 23 scenarios (Table 4-1). The greatest warming is projected for winter at 2.7 °C (0.6 °C to 3.6 °C) and summer at 2.5 °C (1.4 °C to 4.4 °C), with spring and fall both projected to increase by 2.1 °C (1.1 °C to 3.9 °C; Table 4-1). These results are 0.8 °C, 0.7 °C and 0.7 °C warmer than those projected in Rodenhuis et al. (2007) in winter, summer and annually, respectively, because the eight models selected for this study are warmer than the 15 investigated in the Climate Overview. Annual precipitation is projected to increase by 8% (0% to 18%) by the 2050s (Table 4-1). Almost equal increases are projected for winter, spring and fall of ~12% (0% to 27%). Decreases of -1% are projected in summer based on the median, although they could be as great as -21% (minimum) or could increase by 5% (maximum). Projected increases in precipitation annually and seasonally are within 5% of those based on the 15 scenarios in the Climate Overview (Rodenhuis et al. 2009).

Table 4-1. BC 2050s (2041-2070) ensemble temperature and precipitation anomalies from 1961-1990, including 23 downscaled projections from 8 GCMs run under B1, A1B and A2 (except for HADGEM1 which was not available for B1). Values are computed for each projection as averaged over BC.

	Temperature Anomaly (°C)					Precipitation Anomaly (%)				
	Winter	**Spring**	**Summer**	**Fall**	**Annual**	**Winter**	**Spring**	**Summer**	**Fall**	**Annual**
Minimum	0.6	1.1	1.4	1.3	1.4	5	0	-21	1	0
Average	2.6	2.1	2.6	2.2	2.4	13	12	-3	13	9
Median	2.7	2.1	2.5	2.1	2.3	12	13	-1	12	8
Maximum	3.6	3.2	4.4	3.9	3.7	26	19	5	27	18

Seven regions were defined in the Climate Overview to describe the variation in climate across the province: (1) South Coast, (2) Okanagan, (3) Columbia Basin, (4) Fraser Plateau, (5) North Coast, (6) Northwest, and (7) Peace Basin (Figure 4-1). BCSD results have been queried for these basins and will be described here and contrasted to those for the Climate Overview. Average winter temperature increases in the 2050s are projected to be the greatest in the Peace Basin at 3.1°C and the least on the South Coast at

2.0°C (Table 4-2). Temperature increases are almost uniform across the province in spring, ranging from 2.0°C to 2.2°C. During summer, the Columbia and Okanagan basins are projected to warm the most at 3.1°C and 3.2°C, respectively, while the North Coast is projected to warm by only 2.1°C (Table 4-2). Similar to spring, there is less range in the temperature changes projected for fall. The Columbia, Peace and Okanagan basins are projected to warm the most in fall at 2.3°C, 2.3°C and 2.4°C, respectively, based on the ensemble. Annually, the least increase is projected for the North Coast (2.1°C), while the Okanagan, Columbia and Peace Basins all tie for the greatest temperature increase at 2.5°C. These projected increases are larger than those in the Climate Overview, but the pattern of which regions warm more so than others is similar.
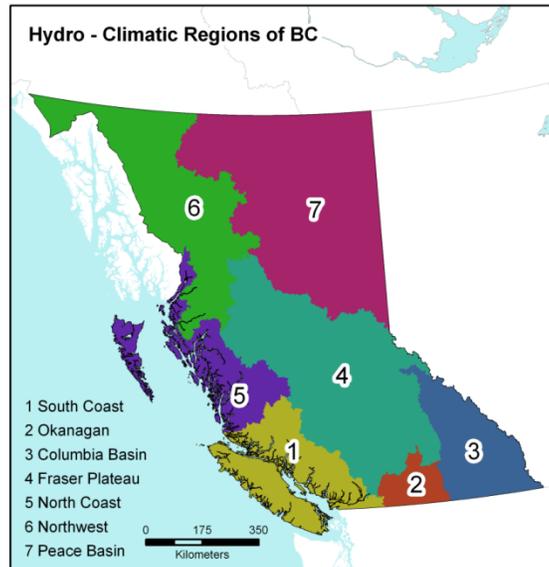
Figure 4-1. Hydro-climatic regions defined for the Climate Overview report (*Rodenhuis et al*. 2009).

Table 4-2. Regional 2050s (2041-2070) ensemble average temperature and precipitation anomalies from 1961-1990, including 23 downscaled projections from eight GCMs run under B1 (except for HADGEM1), A1B and A2.

	Region	Temperature Anomaly (°C)					Precipitation Anomaly (%)				
		Winter	Spring	Summer	Fall	Annual	Winter	Spring	Summer	Fall	Annual
1	**South Coast**	2.0	2.0	2.5	2.1	2.2	5	6	-14	8	4
2	**Okanagan**	2.4	2.2	3.2	2.4	2.5	7	9	-14	9	3
3	**Columbia**	2.4	2.1	3.1	2.3	2.5	13	12	-9	12	8
4	**Fraser**	2.4	2.2	2.6	2.2	2.4	11	11	-7	12	6
5	**North Coast**	2.2	2.0	2.1	2.0	2.1	9	8	-5	9	7
6	**Northwest**	2.7	2.1	2.3	2.2	2.3	15	12	8	13	12
7	**Peace Basin**	3.1	2.2	2.4	2.3	2.5	19	17	4	17	12

The largest increases in winter precipitation for the 2050s are projected for the Peace Basin (19%), while the smallest are projected for the South Coast (5%; Table 4-2). The largest increases in precipitation are projected for winter in all regions, except the Okanagan, South Coast, and Fraser. In the Fraser, the greatest increases are projected for fall. Spring increases are largest in the Peace Basin (17%). Decreases

in precipitation are projected for most areas during summer, except for the Peace Basin and the Northwest, where precipitation is projected to increase by 4% and 8%, respectively. In fall, the largest increases are also projected in the Peace region (17%). Annually, increases in the Peace Basin and in the Northwest region are on par at 12%. Other regions like the South Coast are projected to increase by only 4%.
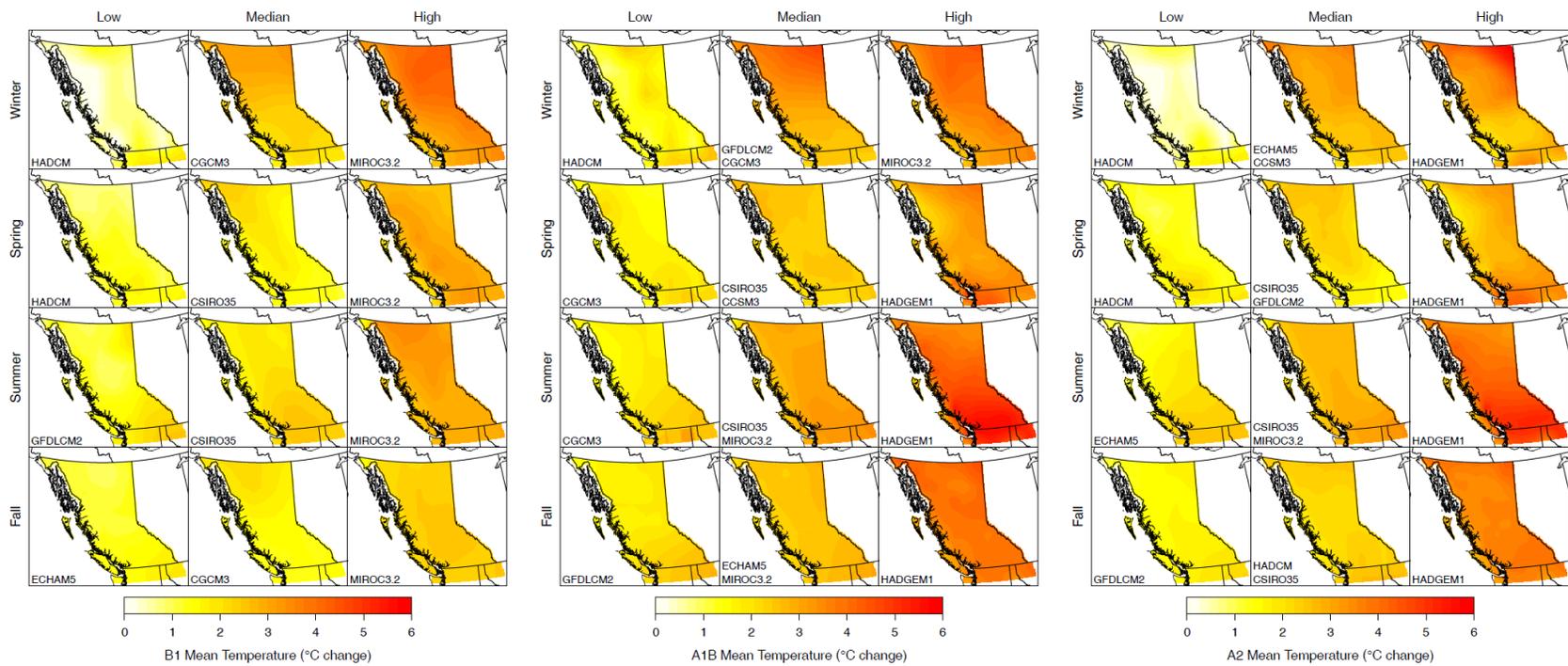
Figure 4-2. Temperature (°C) change projected for the 2050s (2041-2070) from 1961-1990 under the B1, A2 and A1B emissions scenario for each seasons for the low, median and high scenario of BCSD downscaled data from eight selected GCMs (except no HADGEM1_B1).
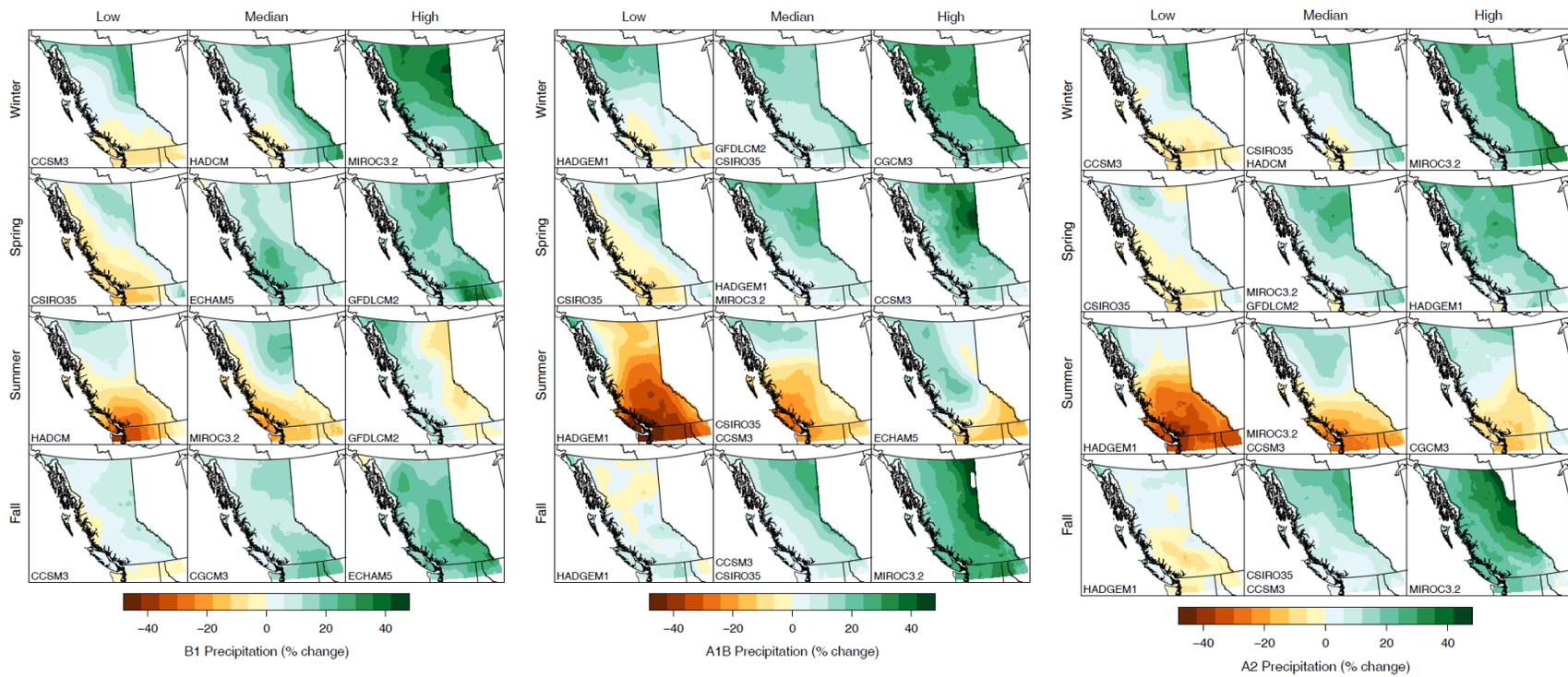
Figure 4-3. Precipitation change as a percentage of 1961-1990 projected for the 2050s (2041-2070) under the B1, A2 and A1B emissions scenario for the low, median and high scenario of BCSD downscaled data from eight selected GCM (except no HADGEM1_B1).

In the following two paragraphs, BCSD results for the province will be explored by emissions scenario annually and by season. The greatest warming in annual temperature is projected by models run under the A1B emissions scenario for minimum, median and maximum scenarios (Table 4-3). The least amount of temperature increase is projected in scenarios run under the B1 emissions scenarios (Table 4-3). The ratio of median increase in annual temperature projected across the province can be stated as 1.00:1.39:1.27 for the B1:A2:A1B emissions scenarios, respectively. Annual precipitation projections for the 2050s are fairly uniform by emissions scenario (Table 4-3). The ratio of median increases in precipitation projected across the province is 1.00:1.13:0.88 for the B1:A2:A1B emissions scenarios, respectively. The widest range in precipitation changes occurs under the A1B emissions scenario where minimum and maximum changes range from 0% to 18% (Table 4-3). Annually, projected precipitation changes vary more from the minimum and maximum of the ensemble (-21% to 5%; Table 4-1) than they do from one emissions scenario to another (0% to 6%; Table 4-3).

Table 4-3. BC 2050s (2041-2070) ensemble annual temperature and precipitation anomalies from 1961-1990 by emissions scenario for BCSD downscaled projections from eight GCMs (except for HADGEM1 which had no B1).

Emissions Scenarios	Temperature Anomaly (°C)			Precipitation Anomaly (%)		
	Min	50th	Max	Min	50th	Max
B1	1.4	**1.8**	2.9	6	**8**	15
A1B	2.2	**2.5**	3.7	0	**9**	18
A2	1.8	**2.3**	3.5	3	**7**	15

Across all seasons, projected changes in temperature and precipitation in the 2050s under the A1B scenario are the greatest on average across BC when compared to the results for models run under B1 and A2 (Table 4-4; Figure 4-2; Figure 4-3). Median warming is greater in winter at 3.2°C than any other season under A1B. The lowest increase in temperature is projected for fall under B1 at 1.6°C. Median projected precipitation change in the 2050s under A1B range from decreases projected for summer (-5%) to increases projected in fall (12%), spring (15%), and winter (13%; Table 4-4). These changes are within 5% of median changes projected under all 23 scenarios (Table 4-1). Under the median of the A1B scenario, precipitation increases of 10% to 20% are projected for winter, spring and fall for most of the province; areas in the northeast are projected to have increases of closer to 30% (Figure 4-3). The largest decreases (-20%) are projected for summer under this scenario and expected to occur in the southern half of the province according to the median of eight GCMs downscaled using BCSD (Figure 4-3).

Table 4-4. BC 2050s (2041-2070) ensemble seasonal temperature and precipitation anomalies from 1961-1990 by emissions scenario for BCSD downscaled projections from eight GCMs (except for HADGEM1 which had no B1).

	Temperature Anomaly (°C)											
	Winter			Spring			Summer			Fall		
Emissions	Min	Median	Max	Min	Median	Max	Min	Median	Max	Min	Median	Max
B1	0.6	2.5	3.6	1.1	1.7	2.8	1.4	2.0	3.0	1.3	1.6	2.3
A1B	1.5	3.2	3.6	1.7	2.4	3.2	1.9	3.0	4.4	1.9	2.5	3.9
A2	0.6	2.9	3.3	1.4	2.1	2.8	1.8	2.7	4.2	1.6	2.2	3.6
	Precipitation Anomaly (%)											
	Winter			Spring			Summer			Fall		
Emissions	Min	Median	Max	Min	Median	Max	Min	Median	Max	Min	Median	Max
B1	6	12	26	0	13	19	-4	0	4	5	12	20
A1B	10	13	26	3	15	19	-21	-5	5	3	12	27
A2	5	8	22	1	14	18	-14	-2	2	1	12	26

Overall, the spatial pattern of projected change was consistent among downscaled models within seasons. In the winter, warming primarily took place in the northern portion of the province (Figure 4-2). In the summer, warming was more concentrated in the southeast. Warming was more uniform over the province in the spring and fall. Precipitation was projected to increase more in the northern and eastern regions of the province during the winter, spring and fall, and to decrease in the southwest during the summer (Figure 4-3). GFDL2.1 run 1 B1 had a different spatial pattern than the other models during summer, where precipitation was projected to decrease in the eastern portion of the province and increase in the west (Figure 4-3).

4.2 Spatial - CGCM3 A2

One of the models selected for downscaling with BCSD was CGCM3. This model is used widely (e.g., Dawson et al. 2008; Picketts et al. 2009; Mote and Salathé 2009; Rodenhuis et al. 2009; PCIC 2010a and PCIC 2010b) and performed well according to the performance metrics presented in section 3.2. Additionally, other studies have recommended this model (Murdock and Spittlehouse, in prep.), or have presented results from this model for BC (Rodenhuis et al. 2009). Results for CGCM3 A2 run1 are shown here to demonstrate how BCSD results differ from that of the GCM in its native resolution. These results will also help to situate the projections from this model amongst the seven other models selected for this study as a relatively warm/cool or wet/dry model relative to the others in the group over the province. In the three BC watersheds mentioned previously, the Campbell, Peace and Upper Columbia, CGCM3 A2 run1 was in the middle of the range of projected changes in temperature and precipitation in the 2050s versus 1961-1990 (Figure 2-1, Figure 2-2 and Figure 2-3).

The mean annual temperature and precipitation for the BCSD results (left panels of Figure 4-4 and Figure 4-5) have a similar range to the un-corrected CGCM3 results (right panels of Figure 4-4 and Figure 4-5). They are equivalent to those presented in the *Climate Overview: Hydro-climatology and Future Climate Impacts in British Columbia* report (Rodenhuis et al. 2009). In both reports, the northern regions of the province are projected to warm the most by ~3°C (Figure 4-4) and the precipitation is projected to increase by up to 30% in the northwest region of the province (Figure 4-5). Temperature changes are fairly uniform across the province in both products. This is because the GCM is coarsely resolved and BCSD does not add detail when temperature differences are examined (2050s Average Temperature minus 1961-1990). The precipitation response in the BCSD downscaled CGCM3 is more spatially resolved, and as a result, the impact of mountain ranges on the precipitation changes can be discerned at this scale. BCSD adjusts the spatial pattern of precipitation change in the GCM to match the gridded-observations in the local scaling step and, unlike temperature, produces smooth maps of precipitation ratios. So when differences are examined in precipitation, there is more regional variation. One area where differences between the two results are dramatic is the southeast portion of the province, where precipitation is projected to increase by ~30% in the BCSD result, whereas precipitation was projected to increase by only ~15% in the un-corrected CGCM3 results. The BCSD technique, which bias corrects each GCM grid against the gridded-observed data aggregated to the GCM scale, adjusts GCMs to have more precipitation in mountainous areas where GCMs would not have the ability to generate it due to lack of elevation gain at low resolution. The BCSD downscaled CGCM3 A2 scenario was second warmest scenario after HADGEM A2 in winter, the third coolest in spring, summer and fall, and the wettest (summer) or second wettest model out of the eight models selected for downscaling in all seasons. Thus, CGCM3 is one of the wetter models of the ensemble and one of the warmest and wettest in winter. Planning made on the basis of CGCM3 may be based on warmer, wetter conditions in winter than other members of the ensemble.

CGCM3 A2 Annual Mean Temperature
2041–2070 minus 1961–1990
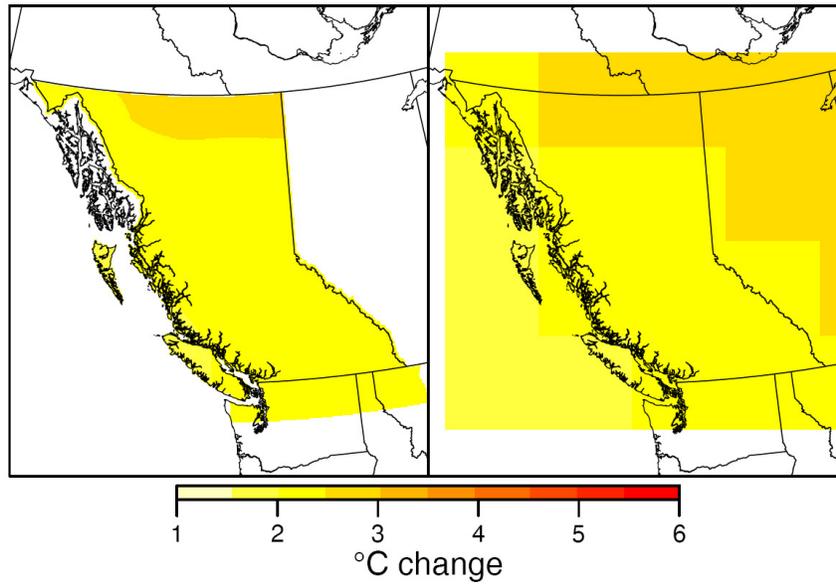
Figure 4-4. BCSD downscaled (left) and raw (right) projected change in annual temperature (°C) for the 2050s (2041-2070) as a difference from 1961-1990 for run 1 of CGCM3 run under the A2 emissions scenario.

CGCM3 A2 Annual Mean Precipitation
2041–2070 minus 1961–1990
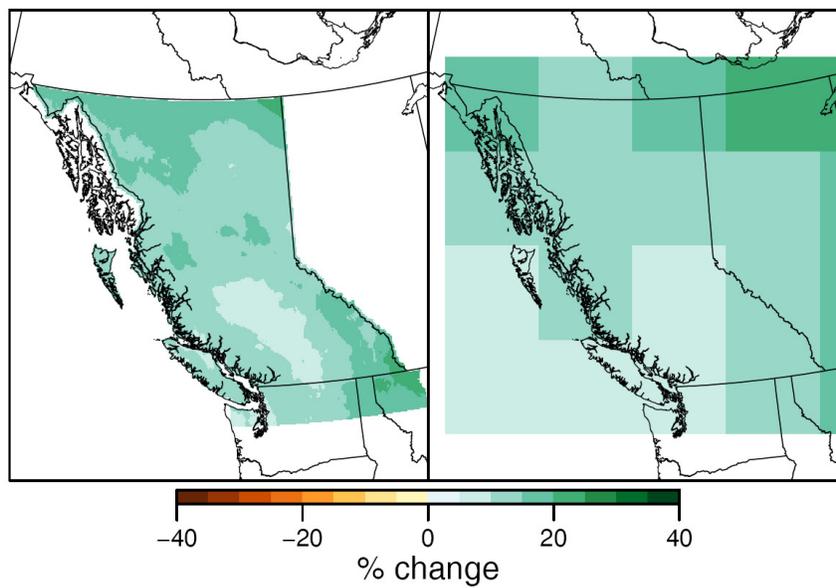
Figure 4-5. BCSD downscaled (left) and raw (right) projected change in annual precipitation (%) for the 2050s (2041-2070) as a difference from 1961-1990 for run 1 of CGCM3 run under the A2 emissions scenario.
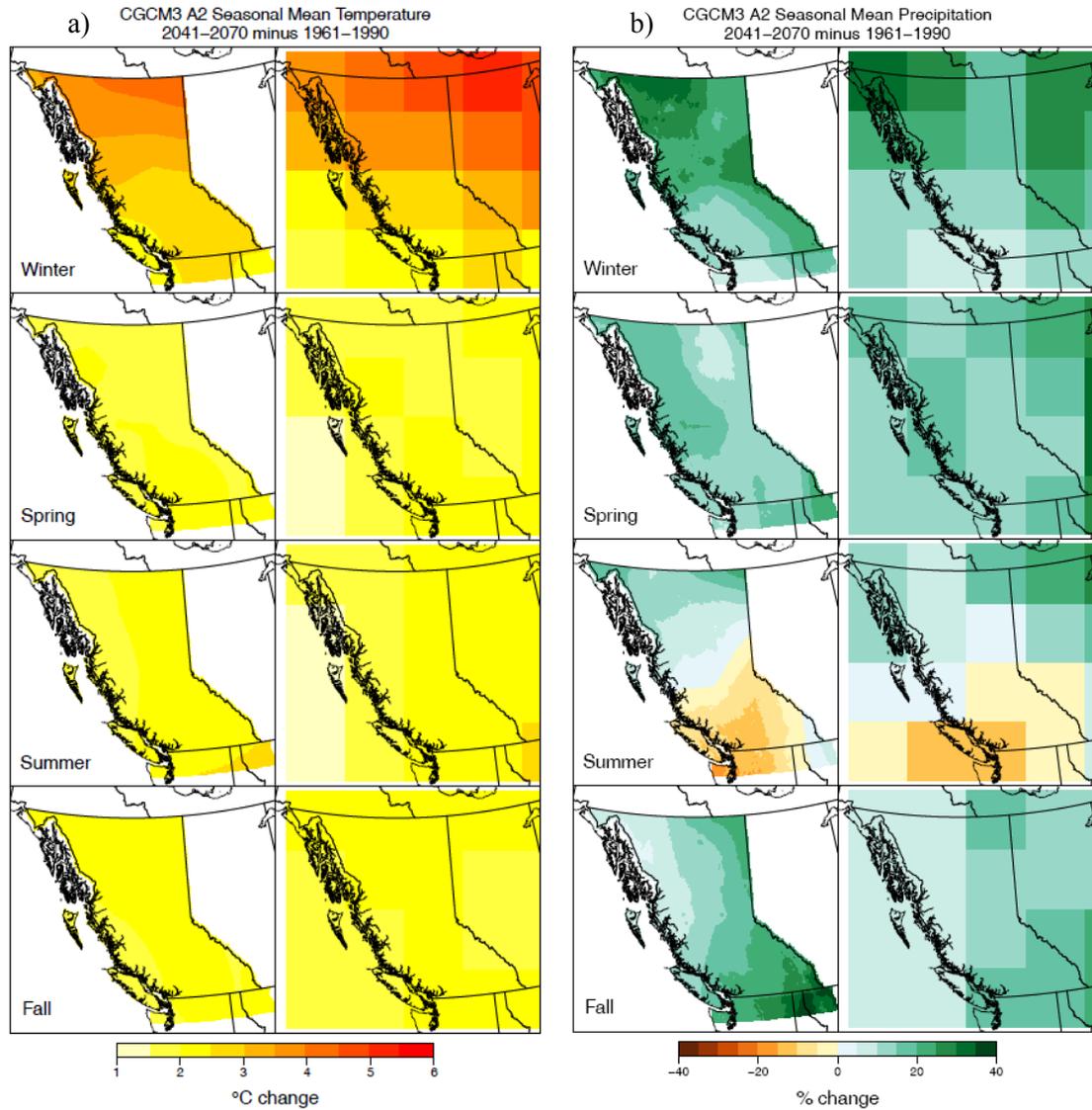
Figure 4-6. BCSD downscaled (left) and raw (right) projected change in seasonal (a) temperature (°C) and (b) seasonal precipitation (%) for the 2050s (2041-2070) as a difference from 1961-1990 for run 1 of CGCM3 run under the A2 emissions scenario.

4.3 Time Series

One of the strengths of the BCSD method is that it generates a bias corrected, spatially disaggregated daily time series at 1/16° resolution for the entire length of available GCM results. BCSD downscaled temperature and precipitation follow the values of the GCM they have been downscaled from closely over the province (Figure 4-7a and Figure 4-7b). In some cases, the smoothing process applied, known as LOESS (Cleveland et al. 1988) has exaggerated the differences between the raw GCM and BCSD results close to 2100. The range in projected temperature and precipitation for the eight selected GCMs is narrower than that of all available GCMs (Table 2-3, Table 2-4, Figure 4-7a and Figure 4-7b). The BCSD results for annual precipitation are slightly wetter over BC than the selected GCMs and then all available GCMs in some decades post 2030, but not consistently over the whole period (Figure 4-7a). Similarly, one model projects more warming than the maximum of the GCM ensemble after 2070 (Figure 4-7a).

Although results are similar between raw GCM output and BCSD results over BC, the BCSD process adjusts projections in sub-regions of the province to better match temperature and precipitation gradients not captured by GCMs that result from elevation changes or proximity to the ocean. On the South Coast, BCSD results are cooler and drier than raw results for CGCM3 A2 run1. In the Peace region, BCSD results are warmer and wetter than raw results for CGCM3 A2 run 1. The trend and variability of projected temperature and precipitation from the GCM is well replicated by BCSD for both regions (Figure 4-8 and Figure 4-9).
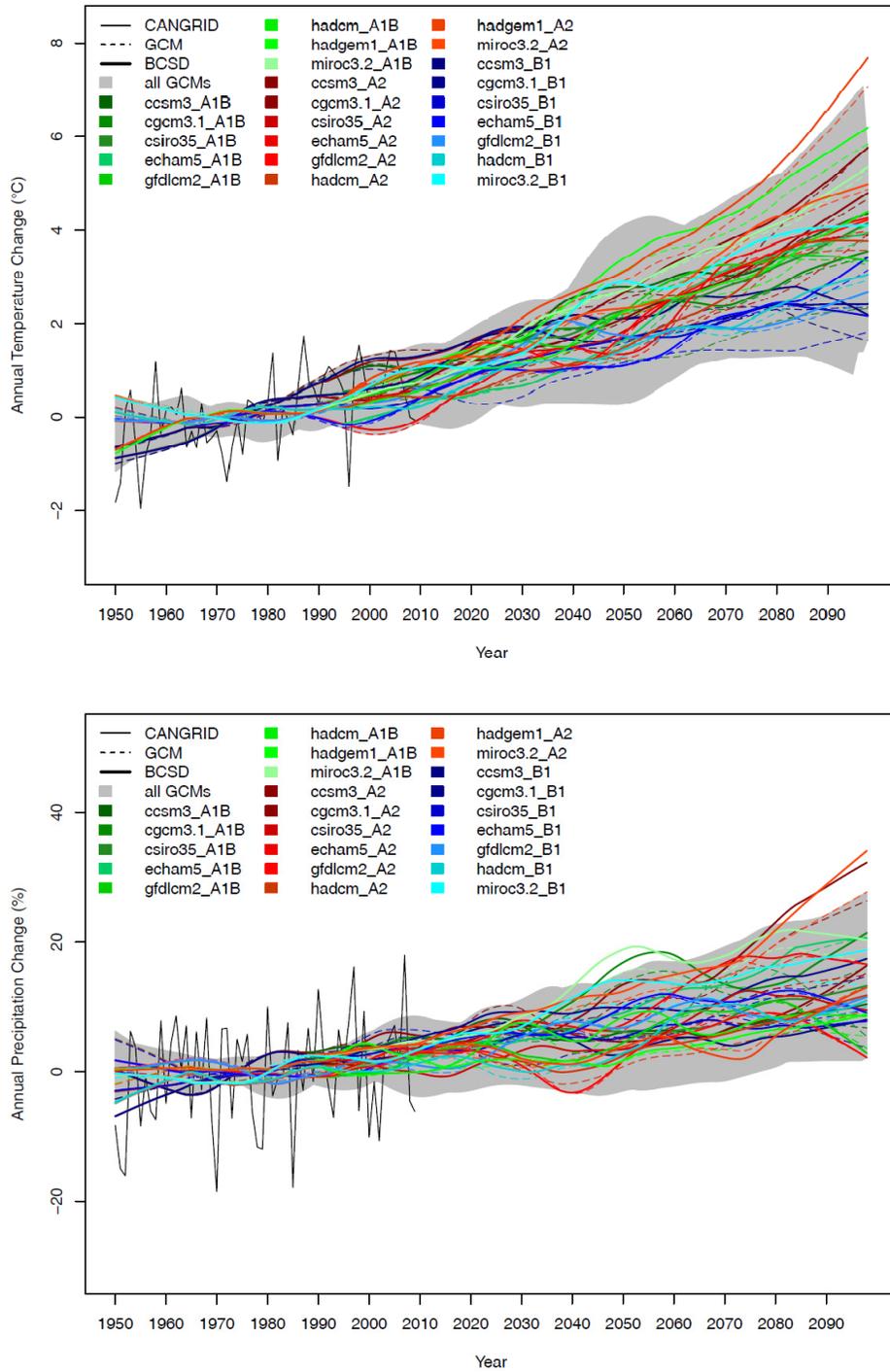
Figure 4-7. Time series (1950-2100) of Global Climate Model (BC average) anomalies from raw selected GCMs (dashed lines) following each of B1, A1B and A2, the Bias Corrected Spatially Disaggregated (BCSD) version (solid lines) of each against the range from all 22 available GCMs (grey swath) for (a) annual mean temperature (b) annual precipitation. Results are smoothed in time using LOESS. CANGRID historical data (black line) is shown for comparison. All results are shown as a difference from their 1961-1990 values.
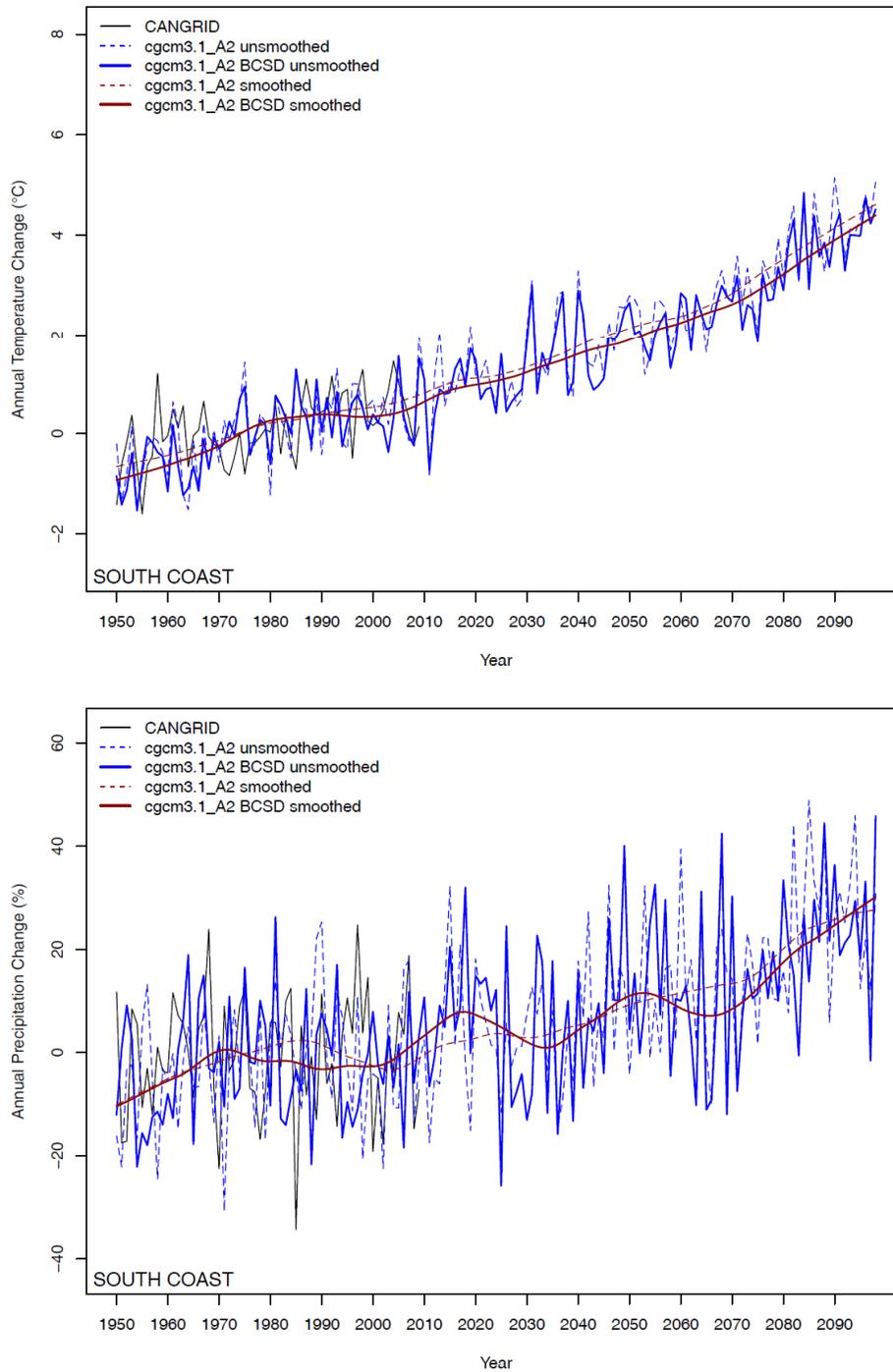
Figure 4-8. Time series (1950-2100) of anomalies from raw selected CGCM3 A2 run1 (dashed line) and the Bias Corrected Spatially Disaggregated (BCSD) CGCM3 A2 run1 (solid line) averaged over the South Coast for (a) annual mean temperature and (b) annual precipitation. Results are shown smoothed in time using LOESS and unsmoothed. CANGRID historical data (black line) is shown for comparison. All results are shown as a difference from their 1961-1990 values.
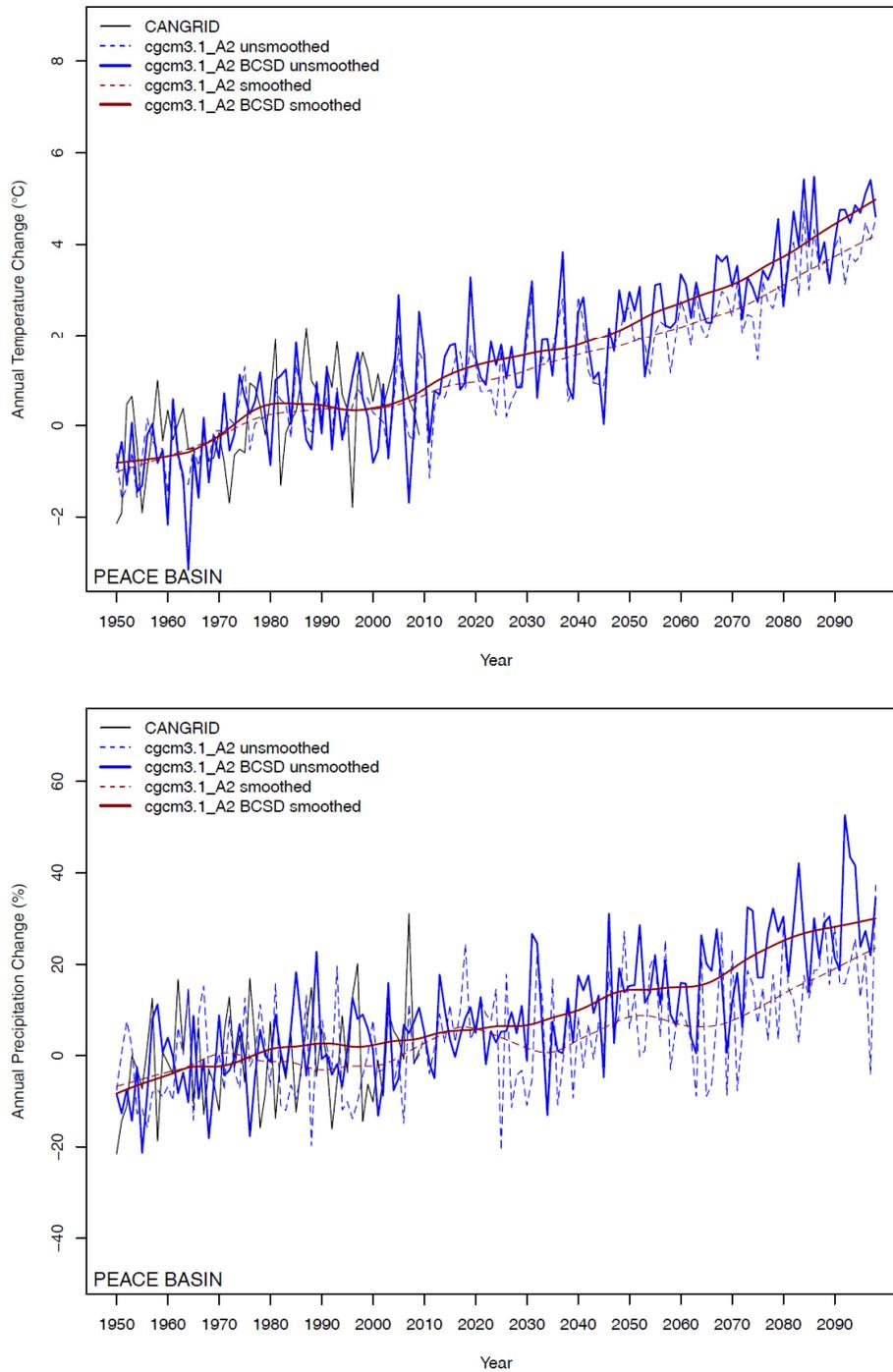
Figure 4-9. Time series (1950-2100) of anomalies from raw selected CGCM3 A2 run1 (dashed line) and the Bias Corrected Spatially Disaggregated (BCSD) CGCM3 A2 run1 (solid line) averaged over the Peace Basin for (a) annual mean temperature and (b) annual precipitation. Results are shown smoothed in time using LOESS and unsmoothed. CANGRID historical data (black line) is shown for comparison. All results are shown as a difference from their 1961-1990 values.

(BLANK)

5. Uncertainty

No one model performs best for all conditions and problems. Uncertainty in these projections is related to the GCM downscaled, the gridded-observations the BCSD process is trained on, and the BCSD process itself. Uncertainties in the GCM are due to: (1) the future climate forcing being unknown, (2) each GCM differing in their response to forcing due to their different parameterizations, and (3) the future trajectory of natural variability being unknown because the sequence of natural variability in each run of a GCM will be slightly different due to small changes in the initial conditions. The gridded-observations the BCSD process bias corrects against is a combination of several different observational networks, each of which contain uncertainty due to measurement errors and quality control protocols. The creation of the gridded-observations depends on the time period it is created for, which alters the stations included or dropped from the scheme. It is also dependent on the digital elevation model used to build it, which has its own uncertainties. The BCSD process makes assumptions about distributions which might not fit all precipitation types and there is a random process of selection of daily values.

Statistical downscaling, such as BCSD, is one of the tools available to translate large-scale GCM information to the local-scale. The value of this technique over uncorrected GCM output is that the regional response of climate change can be better assessed at 1/16°. Its strength over dynamical downscaling approaches is that it can be run on several GCMs without being computationally demanding. Its weaknesses are that it requires long and reliable observed historical data series for calibration, depends on the chosen predictors, does not include feedbacks in the climate system, assumes the established relationship between the predictor and predictand will hold in the future, and maintains the inter-annual variability of the GCM being downscaled which could be different from what we have seen in observations.

Multiple models were selected for downscaling to allow for the range of possible futures to be explored. The range in projected temperatures for models run under one emissions scenario, such as B1, A1B or A2, gives us a sense of the range due to model uncertainty (Table 4-3; Table 4-4; Figure 4-2; Figure 4-3). Annual projected temperature changes can range from 1.8°C (minimum) to 3.5°C (maximum) under the A2 scenario on average over BC, depending on GCM. Thus, from one model to another, the difference in projected change can be as much as 1.7°C. The range for models run under both B1 and A1B is 1.5°C. On a seasonal basis, temperature differences can be even larger between BCSD downscaled GCMs. For example, temperature projections range by 3.0°C between the minimum and maximum values in winter under the A2 scenario (Table 4-4). Part of the difference between ranges for the B1, A1B and A2 scenarios might be attributable to the HADGEM1 model being included in the A2 and A1B ensembles, but not in the B1 ensemble. HADGEM1 is a warmer model that would contribute to an overall increase in projected temperatures. Regardless, all models, run under all emissions scenarios, are in agreement that warming will take place across the province in all seasons (Table 4-4; Figure 4-2).

By comparing the B1, A1B and A2 responses under the median scenario we can get a sense of the range in responses due to emissions scenario. For example, the median annual temperature projection under the A1B scenario is 0.7°C warmer than the B1 scenario on average over BC (Table 4-3). Therefore, the range in annual temperature anomalies from model to model (i.e., 1.7°C) is greater than from emissions scenario to emissions scenario in the 2050s (i.e., 0.7°C). This result would likely change for time periods farther in the future, such as the 2080s, when the difference between emissions scenarios are projected to be greater than during the 2050s (Rodenhuis et al. 2009). Annual precipitation anomalies in the 2050s can range from 0% to 18% under the A1B emissions scenario (Table 4-3). Under the B1 and A2 scenarios ranges are 9% and 12%, respectively. There is 2% or less difference between the median projected changes for the models run under the three emissions scenarios. Clearly, greater range results from multiple GCMs (i.e., 18%) than emissions scenarios on an annual basis (i.e., 2%). On a seasonal basis, there is greater difference between median projected changes from emissions scenario to emissions scenario (up to 5%) and even wider ranges between the minimum and maximum projections (Table 4-8).

(BLANK)

6. Conclusion

Eight Global Climate Models (GCMs) were selected based on their availability, their relative error in representing historic climate over the globe, their performance according to the 'Model Climate Performance Index' (MCPI) over the Northern Hemisphere, and according to the MCPI and the 'Model Variability Index' (MVI) over North America and western North America. The correlation of models to sea level pressure in North American Regional Reanalysis (NARR) based on Self Organizing Maps over North America was also considered. Models were preferred if they were one of the 15 models used by PCIC in the Climate Overview report and one of the five models currently being used in the North American Regional Climate Change Assessment Program (NARCCAP). As a result of this selection process the following GCMS were chosen: CGCM3.1 (T47); CSIRO-Mk3.0; CCSM3; GFDL-CM2.1; MIROC3.2 (medres); ECHAM/MPI-OM; UKMO-HadCM3; and UKMO-HadGEM1. UKMO-HadGEM1 did not meet the selection criteria that the other seven models had, but was included because it had been used for several similar studies. These models are some of the warmer models available and also the same models chosen by similar studies in North America.

Projections of daily minimum and maximum temperature and precipitation for BC at 1/16° have been created for eight GCMs run under the B1, A1B, and A2 emissions scenarios, except HADGEM1 which did not have B1. These daily data can be used to drive secondary models to assess the impacts of climate change on biophysical features such as streamflow or tree species suitability. In comparing National Centers for Environmental Prediction-National Center for Atmospheric Research (NCEP/NCAR) Bias Corrected Spatial Disaggregation (BCSD) downscaled results to gridded-observed data at the 1/16° grid-scale over BC for the validation period (1991-2000), median temperature differences between the two were -0.3°C in July and -0.6°C in December. For precipitation, BCSD downscaled NCEP results produced differences of -4% of gridded-observations based on the median in July and 0% in December. Overall, results were representative of observed average temperature and total precipitation for July and December based on the median bias between BCSD-downscaled NCEP and gridded-observations. It should be noted that this technique does not maintain spatial correlations between temperature and precipitation as these are correct independently at the GCM resolution using quantile mapping.

When comparing daily downscaled NCEP results to daily gridded-observations they matched the explained variance of the gridded-observations at the 99% confidence level for several temperature and precipitation indices. This is only one test of daily values produced by the BCSD method. Station data is not directly comparable spatially averaged gridded downscaled results or gridded-observations. Since the daily values are derived by resampling the historical gridded observations and adjusting them based on the bias-corrected, locally-scaled monthly GCM projections, this approach does not explicitly capture changes to daily extremes that are projected by the various GCMs. In studies that require future daily data to analyze droughts or flood events, other downscaling methods should be sought.

Based on the median results of the 23 BCSD downscaled scenarios, temperature and precipitation are projected to change as follows by the 2050s when compared to 1961-1990.

On average over BC:

- Annually, temperature is projected to increase by 2.3°C and precipitation is projected to increase by 8%.
- Warming is projected to be greatest in winter at 2.7°C and least in spring and fall at 2.1°C.
- Precipitation increases are projected to be greatest in spring at 13% and decreases are projected for summer (-1%).

51

By region:

- Annually, the Okanagan, Columbia and Peace Basins are projected to have the greatest temperature increases (2.5°C), while the Northwest and Peace Basin are projected to have the largest precipitation increases (12%).
- In the winter, the greatest warming is projected for the Peace Basin (3.1°C), while in summer the greatest warming is projected for the Okanagan (3.2°C).
- In the spring and fall, projected warming is relatively uniform across all regions.
- Precipitation is projected to increase the most out of any region in the Peace Basin in all seasons except summer. Projected increases in this basin are for 19% in winter and 17% in spring and fall.
- Decreases are projected during summer in the South Coast, Okanagan, Columbia, Fraser, and North Coast, while increases are projected in the Northwest (8%) and Peace Basin (4%). The largest projected decrease (-14%) is projected for both the South Coast and Okanagan.
- The Northwest and Peace Basin are the only two regions where precipitation is projected to increase in all seasons.

Overall, the spatial pattern of projected change was consistent between downscaled models within seasons. In the winter, warming primarily takes place in the northern portion of the province. In the summer, warming is more concentrated in the southeast. Warming is uniform over the province in the spring and fall. Precipitation is projected to increase more in the northern and eastern regions of the province during the winter, spring and fall, and to decrease in the southwest during the summer. GFDL2.1 run 1 B1 has a different spatial pattern than the other models during summer, where precipitation is projected to decrease in the eastern portion of the province and increase in the west.

When compared to the Climate Overview results, projections made by the eight GCMs selected in this study and downscaled with BCSD are warmer than those presented in the Climate Overview. This is likely due to the cooler models used in the Climate Overview being eliminated in the selection process.

To test the benefits of using BCSD to downscale a GCM, BCSD results for CGCM3 A2 were compared to those of the un-corrected CGCM3 A2. The BCSD process was found to improve the ability of the CGCM3 model to represent the variability in precipitation across the province while maintaining the spatial pattern of change projected by CGCM3, but altered the projections of temperature change very little. Annual projected increases in temperature from the BCSD downscaled CGCM3 A2 scenario are close to the median of the eight BCSD downscaled models. Annual projected precipitation increases are closest to the wettest, second only to MIROC3.2 (medres) A2. The BCSD downscaled CGCM3 A2 scenario is the second warmest scenario after HADGEM A2 in winter, the third coolest in spring, summer and fall and the wettest (summer) or second wettest model out of the eight models selected for downscaling in all seasons. Thus, CGCM3 is one of the wetter models of the ensemble and one of the warmest and wettest in winter.

The contribution to the range of uncertainty of GCMs versus emissions scenarios for the 2050s was investigated by downscaling several GCMs, run under several emissions scenarios. The range between temperature and precipitation projections is greater for the multiple GCMs than it is for emissions scenarios both annually, and seasonally. The range in seasonal response between models is greater than the range in annual response. Given this, to limit the number of scenarios applied to impact modelling it would be more important to use multiple models than it would be to use multiple emissions scenarios in the 2050s. For the 2050s, the difference between projected changes for each emissions scenario is minimal. The course we are currently following exceeds the A2 scenario, which is the least optimistic of the three: B1, A1B and A2 when looking out to 2100.

7.   Future Work

Future work should include downscaling multiple runs of the same GCM using BCSD to test the influence of initial conditions in a given GCM on future projections. Additionally, BCSD should be used to downscale RCMs in BC. This approach removes the majority of the bias inherent in RCM outputs while maintaining the added information from the higher resolution physical-based projection of the RCM. When a hydrologic model was driven with BCSD downscaled RCM and GCM results over the Columbia River Basin, RCM-derived hydrology was found to be more sensitive to climate change than the GCM-derived hydrology (Wood et al. 2004).

Currently, work is underway to increase the resolution of runs with the Canadian Regional Climate Model (CRCM) over BC to take the resolution from 45 km to 15 km a side. This will allow several simulations over the province to be compared to test the influence of initial conditions and the range in possible futures derived from one RCM. Little of this work has been done in BC to date. BC proves to be a challenging province to model with RCMs due to its elevation gradients and ocean influence. Results will help to increase confidence in the dynamical downscaling conducted over BC.

In the case of the BCSD downscaling technique, daily data is created by resampling the observed historic record and adjusting it with bias corrected monthly GCM data. Therefore, changes to daily extremes are an artifact of changes to monthly statistics. The number of days with or without precipitation comes from re-sampling the historical record and is not a result of daily information from the GCM. Thus, daily extremes are not shown here and further studies which apply this data should consider its application primarily in cases where changes to monthly statistics are sought. In the future, more daily GCM data will be made available through the PCMDI for the IPCC Fifth Assessment Report. If this is the case, BCSD could be adapted to work with daily data. Alternatively, where changes in extremes are the primary question, other downscaling techniques might be applied, such as expanded downscaling (Bürger 1996; Bürger et al. 2009) or TreeGEN (Stahl et al. 2008), both of which downscale daily GCM data. However, neither approach is applicable for gridded fields nor over large domains like BC; instead they are conducted to individual stations on a per project basis. In the future, the availability of RCM data will also improve through the CORDEX programme: http://wcrp.ipsl.jussieu.fr/RCD_CORDEX.html allowing the range of uncertainty caused by different driving GCMs and RCMs to be explored more fully.

(BLANK)

References

Annan, J.D., and J.C. Hargreaves, 2010: Reliability of the CMIP3 ensemble. *Geophysical Research Letters*, 37, L02703, doi: 10.1029/2009GL041994

Bennett, K.E., A.T. Werner, and M. Schnorbus, 2009: Uncertainties in hydrologic and climate change impact analyses in a headwater basin of the Peace River watershed. In: Proceedings of the 17th International Northern Research Basins Symposium and Workshop, Iqaluit-Pangnirtung-Kuujjuaq, Canada, August 12-18, 2009.

Bonsal, B.R., T.D. Prowse, and A. Pietroniro, 2003: An assessment of global climate model-simulated climate for the western cordillera of Canada (1961-90). *Hydrological Processes,* 17 (3703-3716).

Brekke, L.D., M.D. Dettinger, E.P. Maurer and M. Anderson, 2008: Significance of model credibility in estimating climate projection distributions for regional hydroclimatoloigcal risk assessments. *Climatic Change*, 89: 371-394.

Bürger, G., 1996: Expanded downscaling for generating local weather scenarios, *Climatic Research*, 7, 111–128.

Bürger, G., D. Reusser, and D. Kneis, 2009: Early flood warnings from empirical (expanded) downscaling of the full ECMWF Ensemble Prediction System, *Water Resources Research*, 45(10), W10443.

Christensen, J.H., B. Hewitson, A. Busuioc, A. Chen, X. Gao, I. Held, R. Jones, R.K. Kolli, W.-T. Kwon, R. Laprise, V. Magaña Rueda, L. Mearns, C.G. Menéndez, J. Räisänen, A. Rinke, A. Sarr and P. Whetton, 2007: Regional Climate Projections. *Climate Change 2007: The Physical Science Basis. Contribution of Working Group I to the Fourth Assessment Report of the Intergovernmental Panel on Climate Change* [Solomon, S., D. Qin, M. Manning, Z. Chen, M. Marquis, K.B. Averyt, M. Tignor and H.L. Miller (eds.)]. Cambridge University Press, Cambridge, United Kingdom and New York, NY, USA.

Cleveland, W.S. and Devlin, S.J., 1988: Locally Weighted Regression: An Approach to Regression Analysis by Local Fitting. *Journal of the American Statistical Association*, 83: 596-610.

Climatic Change, Rodenhuis, D.R., Bennett, K.E., Werner, A.T., Murdock, T.Q., Bronaugh, D. revised 2009: Hydro-climatology and future climate impacts in British Columbia. Pacific Climate Impacts Consortium, University of Victoria, Victoria BC, 132 pp.

Daly, C., R.P. Neilson, and D.L. Philips, 1994: A statistical-topographic model for mapping climatological precipitation over mountainous terrain. *Journal of Applied Meteorology*, 33: 140-158.

Dawson, R., A.T. Werner, T.Q. Murdock, 2008: Preliminary Analysis of Climate Change in the Cariboo-Chilcotin Area of British Columbia. Pacific Climate Impacts Consortium, University of Victoria, Victoria BC, 49 pp.

Easterling, D. R., T. R. Karl, J. H. Lawrimore, and S. A. Del Greco, 1999: United States Historical Climatology Network Daily Temperature, Precipitation, and Snow Data for 1871-1997. ORNL/CDIAC-118, NDP-070. Carbon Dioxide Information Analysis Center, Oak Ridge National Laboratory, U.S. Department of Energy, Oak Ridge, Tennessee.

Flower, A., Murdock, T.Q., Taylor, S., Zwiers, F.W., submitted: Using an ensemble of downscaled climate model projections to assess impacts of climate change on the potential distribution of spruce and Douglas-fir forests in British Columbia. *Journal of Environmental Science and Policy*.

Fowler, H.J., S. Blenkinsop, and C. Tebaldi, 2007: Review: Linking climate change modelling to impacts studies: recent advances in downscaling techniques for hydrological modelling. *International Journal of Climatology*, 27: 1547-1578.

Gleckler P J, Taylor K E, Doutriaux C. 2008: Performance metrics for climate models. *Journal of Geophysical Research*, 113: DO6104. DOI: 10.1029/2007JD008972.

Hamann, A. and T.L. Wang, 2005: Models of climatic normals for genecology and climate change studies in British Columbia, *Agricultural and Forest Meteorology*, 128: 211-221.

Hamlet, A.F. and D.P. Lettenmaier, 1995: Production of temporally consistent gridded precipitation and temperature fields for the continental United States. *Journal of Hydrometeorology*, 6: 330-336.

Hamlet, A.F., P. Carrasco, J. Deems, M.M. Elsner, T. Kamstra, C. Lee, S-Y Lee, G. Mauger, E. P. Salathe, I. Tohver, L. Whitely Binder, 2010: Final Project Report for the Columbia Basin Climate Change Scenarios Project, http://www.hydro.washington.edu/2860/report/".

Hawkins, E., and R. Sutton, 2009: The potential to narrow uncertainty in regional climate predictions. *Bulletin of the American Meteorological Society*, 1095-1107.

Hay, L.E., M.P. Clark, 2003: Use of statistically and dynamically downscaled atmospheric model output for hydrologic simulations in three mountainous basins in the western United States. *Journal of Hydrology*, 282: 56-75.

Haylock, M.R., N. Hofstra, A.M.G. Klien Tank, E.J. Klok, P.D. Jones and M. New, 2008: A European daily high-resolution gridded data set of surface temperature and precipitation for 1950-2006. *Journal of Geophysical Research*, 113: 1-12.

Hegerl, G.C., F. W. Zwiers, P. Braconnot, N.P. Gillett, Y. Luo, J.A. Marengo Orsini, N. Nicholls, J.E. Penner and P.A. Stott, 2007: Understanding and Attributing Climate Change. In: Climate Change 2007: The Physical Science Basis. Contribution of Working Group I to the Fourth Assessment Report of the Intergovernmental Panel on Climate Change [Solomon, S., D. Qin, M. Manning, Z. Chen, M. Marquis, K.B. Averyt, M. Tignor and H.L. Miller (eds.)]. Cambridge University Press, Cambridge, United Kingdom and New York, NY, USA.

Hughes, P. Y., E. H. Mason, T. R. Karl, and W. A. Brower, 1992: United States Historical Climatology Network Daily Temperature and Precipitation Data. ORNL/CDIAC-50, NDP-042. Carbon Dioxide Information Analysis Center, Oak Ridge National Laboratory, U.S. Department of Energy, Oak Ridge, Tennessee.

IPCC, 2007a: *Climate Change 2007: The Physical Science Basis*. Contribution of Working Group I to the Fourth Assessment Report of the Intergovernmental Panel on Climate Change [Solomon, S., D. Qin, M. Manning, Z. Chen, M. Marquis, K.B. Averyt, M. Tignor and H.L. Miller (eds.)]. Cambridge University Press, Cambridge, United Kingdom and New York, NY, USA, 996 pp.

IPCC, 2007b: Summary for Policymakers. In *Climate change 2007: The Physical Science Basis.* Contribution of Working Group I to the Fourth Assessment of the Intergovernmental Panel on Climate Change, Solomon S et al. (eds). Cambridge University Press: Cambridge. U.K; 1-18.

IPCC, 2008: *http://www.ipcc-data.org/ddc_gcm_guide.html. (Page last modified:* 26 November 2008).

Kalnay, E.; Kanamitsu, M.; Kistler, R.; Collins, W.; Deaven, D.; Gandin, L.; Iredell, M.; Saha, S.; White, G.; Woollen, J.; Zhu, Y.; Chelliah, M.; Ebisuzaki, W.; Higgins, W.; Janowiak, J.; Mo, K.C.; Ropelewski, C.; Wanj, J.; Leetmaa, A.; Reynolds, R.; Jenne, R.; Joseph, D. 1996: The NCEP/NCAR 40-year reanalysis project. *Bulletin of the American Meteorological Society,* 77:437–471.

Knutti, R., G. Abramowitz, M. Collins, V. Eyring, P.J. Gleckler, B. Hewiston, and L. Mearns, 2010: Good practice guidance paper on assessing and combining multi model climate projections. In: *Meeting Report of the Intergovernmental Panel on Climate Change expert meeting on assessing and combining multi model climate projections*, Stocker, T.F., D. Qin, G, -K. Plattner, M. Tignor, and P.M. Midgley (eds.). IPCC Working Group I Technical Support Unit, University of Bern, Bern, Switzerland.

Knutti, R., R. Furrer, C. Tebaldi, J. Cermak and G.A. Meehl, 2010: Challenges in combining projection distributions for regional hydroclimatological risk assessments, *Climatic Change*, 89(3-4): 371-394.

Leduc M, Laprise R. 2010: Quantifying climate change signal and spread from an "ensemble of opportunity." 44th Annual Canadian Meteorological and Oceanographic Society (CMOS) Congress, Ottawa, Canada.

Leung, L.R., L.O. Mearns, F. Giorgi and R.L. Wilby, 2003: Regional Climate Research. *Bulletin of the American Meteorological Society*, 84(1): 89-95.

Liang, X., D.P. Lettenmaier and E.F. Wood, 1994: A simple hydrologically based model of land surface water and energy fluxes for general circulation models. *Journal of Geophysical Research*, 99(D7): 14, 415-14, 428

Maraun, D., F. Wetterhall, A.M. Ireson, R.E. Chandler, E.J. Kendon, M. Widmann, S. Brienen, H.W. Rust, T. Sauter, M. Themeßl, V.K.C. Venema, K.P. Chun, C.M. Goodess, R.G. Jones, C. Onof, M. Vrac and I, Thiele-Eich, 2010: Precipitation downscaling under climate change: recent developments to bridge the gap between dynamical models and the end user. 48 (RG3003): 1-34.

Maurer, E.P. and H.G. Hidalgo, 2008: Utility of daily vs. monthly large-scale climate data: an intercomparison of two statistical downscaling methods. *Hydrology and Earth System Sciences*, 12: 551-563.

Maurer, E.P., A.W. Wood, J.C. Adam, D.P. Lettenmaier, and B. Nijssen, 2002: A long-term hydrologically based dataset of land surface fluxes and states for the conterminous United States. *Journal of Climate*, 15: 3237-3251.

Meehl, G.A., C. Covey, T. Delworth, M. Latif, B. McAvaney, J.F.B. Mitchell, R.J. Stouffer and K.E. Taylor, 2007: The WCRP CMIP3 Multimodel Dataset: A new era in climate change research. *Bulletin of the American Meteorological Society*, 88(9): 1383-1394.

Mekis, É. and W.D. Hogg, 1999: Rehabilitation and analysis of Canadian daily precipitation time series. *Atmosphere-Ocean*, 37:53–85.

Mote, P.W. and E.P. Salathé Jr., 2009: Future Climate in the Pacific Northwest, Chapter 1: Scenarios. Pgs. 21-43.

Moore, R.D., Jost, G., Clarke, G.K.C, Anslow, F., Radic, V., Menounos, B., Wheate, R., Werner, A., and Murdock, T., 2010: Glacier and streamflow response to future climate scenarios, Mica Basin, British Columbia. November 15th 2010. Draft Final Report Prepared for BC Hydro, University of British Columbia, University of Northern British Columbia, Pacific Climate Impacts Consortium. 144 pp.

Moore et al., 2010: Glacier and Streamflow Response to Future Climate Scenarios, Mica Basin, British Columbia. Draft Final Report Prepared for BC Hydro. 15 November 2010, R.D. Moore, G. Jost, (Department of Geography, The University of British Columbia) G.K.C. Clarke, F. Anslow, V. Radic (Department of Earth and Ocean Sciences, The University of British Columbia) B. Menounos, R. Wheate (Geography Program, University of Northern British Columbia), A.T. Werner, T.Q. Murdock, Pacific Climate Impacts Consortium, Victoria. 138 pp.

Murdock, T.Q., Flower, A., 2009: Final Technical Report Forest Science Program Project # Y093061 Development and analysis of forest health databases, models, and economic impacts for BC: Spruce bark beetle & spruce; western spruce budworm and Douglas fir, Pacific Climate Impacts Consortium, University of Victoria, Victoria, BC.

Murdock and Spittlehouse, 2011: Selecting and Using Climate Change Scenarios for British Columbia, Pacific Climate Impacts Consortium, University of Victoria, Victoria, BC. 32 pp.

Nelson, H., 2010: Validating Impacts, Exploring Vulnerabilities, and Developing Robust Adaptive Strategies under the Kamloops Future Forest Strategy (File: 012_Nelson). Future Forest Ecosystems Scientific Council (FFESC) Interdisciplinary Climate Change Adaptation Research for Forest and Rangeland Ecosystems 2009-10 Year End Progress Report. Forest Resources Management, University of British Columbia. 89 pp.

Overland, J.E. and Wang, M., 2007: Future regional Arctic sea ice declines, *Geophysical Research Letters*, 34:1-7.

PCIC, 2010a: http://pacificclimate.org/tools/select

PCIC, 2010b: http://plan2adapt.ca/

PCMDI, 2010: Lawrence Livermore National Laboratory's Program for Climate Model Diagnosis and Intercomparison, accessed December, 2010. http://www-pcmdi.llnl.gov/ipcc/about_ipcc.php

Peterson, T. C., 2005: Climate change indices, *WMO Bulletin*, 54(2), 83–86.

Picketts, I.M., A.T. Werner and T.Q. Murdock, 2009: Climate change in Prince George: summary of past trends and future projections. Pacific Climate Impacts Consortium, University of Victoria, Victoria BC, 48 pp.

Pierce D W, Barnett T P, Santer B D, Gleckler P J. 2009: Selecting global climate models for regional climate change studies. *Proceedings of the National Academy of Sciences*, 106(21): 8441-8446.

Pincus R, Batstone C P, Hofmann R J P, Taylor K E, Gleckler P J. 2008: Evaluating the present-day simulation of clouds, precipitation, and radiation in climate model. *Journal of Geophysical Research*, 113: D14209. DOI: 10.1029/2007JD009334.

Pope, V, 2007: UK Met Office's Hadley Centre, Published: 2007/02/02 00:23:46 GMT http://news.bbc.co.uk/go/pr/fr/-/2/hi/science/nature/6320515.stm.

Randall, D.A., R.A. Wood, S. Bony, R. Colman, T. Fichefet, J. Fyfe, V. Kattsov, A. Pitman, J. Shukla, J. Srinivasan, R.J. Stouffer, A. Sumi and K.E. Taylor, 2007: Climate Models and Their Evaluation. *Climate Change 2007: The Physical Science Basis*. Contribution of Working Group I to the Fourth Assessment Report of the Intergovernmental Panel on Climate Change [Solomon, S., D. Qin, M. Manning, Z. Chen, M. Marquis, K.B. Averyt, M.Tignor and H.L. Miller (eds.)]. Cambridge University Press, Cambridge, United Kingdom and New York, NY, USA.

Rodenhuis, D., Bennett, K., Werner, A., Murdock, T.Q. and Bronaugh, D., 2009: Hydro-climatology and Future Climate Impacts in British Columbia (revised). Pacific Climate Impacts Consortium, University of Victoria, 132 pp.

Rodenhuis, D., Braun, M., Music, B., Caya, D, 2011: Climate diagnostics of future water resources in BC watersheds, Hydrologic Impacts. Pacific Climate Impacts Consortium, University of Victoria. 74 pp.

Rougier, J.C, M. Goldstein, and L. House, 2010: Assessing climate uncertainty using evaluations of several different climate simulators. http://www.maths.bris.ac.uk/~MAZJCR/mme2.pdf

Rummukainen, M., 1997: Methods for statistical downscaling of GCM simulation. SWECLIM report. Norrköping: Rossby Centre, SMHI.

Salathé, E.P., 2003: Comparison of various precipitation downscaling methods for the simulation of streamflow in a rainshadow river basin. *International Journal of Climatology,* 23: 887–901.

Salathé, E.P., 2005: Downscaling simulations of future global climate with application to hydrologic modelling. *International Journal of Climatology*, 25: 419-436.

Salathé, E.P., P.W. Mote, and M.W. Wiley, 2007: Review of scenario selection and downscaling methods for the assessment of climate change impacts on hydrology in the United States pacific northwest. *International Journal of Climatology*, 27: 1611-1621.

Schnorbus, M.A., K.E. Bennett, A.T. Werner and A.J. Berland, 2011: Hydrologic Impacts of Climate Change in the Peace, Campbell and Columbia Watersheds, British Columbia, Canada. Pacific Climate Impacts Consortium, University of Victoria, Victoria, BC. 157 pp.

Shepard, D. S., 1984: Computer mapping: The SYMAP interpolation algorithm. *Spatial Statistics and Models*, G. L. Gaile and C. J. Willmott, Eds., D. Reidel, 133–145.

Stahl, K., R. D. Moore, J. M. Shea, D. Hutchinson, and A. J. Cannon, 2008: Coupled modelling of glacier and streamflow response to future climate scenarios, *Water Resources Research*, 44(2), W02422.

Tebaldi, C., and R. Knutti, 2007: The use of the multi-model ensemble in probabilistic climate projections. *Philosophical Transactions of the Royal Society: Series A*, 365: 2053-2075.

Vincent, L.A. and D.W. Gullett, 1999: Canadian historical and homogeneous temperature datasets for climate change analysis. *International Journal of Climatology,* 12: 1975-1388.

Wang, T., Hamann, A., Spittlehouse, D., and Aitken, S. N. 2006: Development of scale-free climate data for western Canada for use in resource management. *International Journal of Climatology*, 26(3):383-397.

Weart, S. "The Discovery of Global Warming" Harvard University Press, Revised Edition, 2008: USA. 240 pp.

Wehner, M.F., R.L. Smith, G. Bala and P. Duffy, 2010: The effect of horizontal resolution on simulation of very extreme US precipitation events in a global atmosphere model. *Climate Dynamics*, 34: 241-247.

Wilby, R.L. and T.M.L.Wigley , 1997: Downscaling general circulation model output: a review of methods and limitation. *Progress in Physical Geography,* 21: 530-548.

Wilby, R.L., L.E. Hay, W.J.J. Gutowski, R.W. Arritt, E.S. Tackle, Z. Pan, GH. Leavesley, and MP. Clark, 2000: Hydrological responses to dynamically and statistically downscaled climate model output. *Geophysical Research Letters*, 27: 1199-1202.

Wood, A.W., E.P. Maurer, A. Kumar and D.P. Lettenmaier, 2002: Long-range experimental hydrologic forecasting for the eastern United States. *Journal of Geophysical Research*, 107: 1-15.

Wood, A.W., L.R. Leung, V. Sridhar and D.P. Lettenmaier, 2004: Hydrologic implications of dynamical and statistical approaches to downscaling climate model outputs. *Climatic Change*, 62: 189-216.

Xu, C., 1999: From GCMs to river flow: a review of downscaling methods and hydrologic modelling approaches. *Progress in Physical Geography*, 23: 229-249.

(BLANK)

List of Figures

List of Tables